

BSC


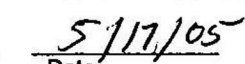
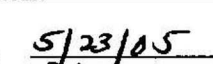
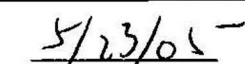
Scientific Analysis Administrative Change Notice

QA: QA

Page 1 of 5

Complete only applicable items.

1. Document Number:	ANL-NBS-MD-000001	2. Revision:	03	3. ACN:	01
4. Title:	Features, Events, and Processes in UZ Flow and Transport				
5. No. of Pages Attached:	58				

6. Approvals:	
Preparer:	<div style="display: flex; justify-content: space-between;"> <div> <u>G.H. Nieder-Westermann</u> Print Name and Sign </div> <div> SIGNATURE ON FILE  </div> </div> <div style="display: flex; justify-content: flex-end; margin-top: -20px;"> Date <u>05/17/05</u> </div>
Checker:	<div style="display: flex; justify-content: space-between;"> <div> <u>Jim Houseworth</u> Print name and sign </div> <div> SIGNATURE ON FILE  </div> </div> <div style="display: flex; justify-content: flex-end; margin-top: -20px;"> Date <u>5/17/05</u> </div>
QER:	<div style="display: flex; justify-content: space-between;"> <div> <u>Judy Gebhart</u> Print name and sign </div> <div> SIGNATURE ON FILE  </div> </div> <div style="display: flex; justify-content: flex-end; margin-top: -20px;"> Date <u>5/23/05</u> </div>
Responsible Manager:	<div style="display: flex; justify-content: space-between;"> <div> <u>Ming Zhu</u> Print name and sign </div> <div> SIGNATURE ON FILE  </div> </div> <div style="display: flex; justify-content: flex-end; margin-top: -20px;"> Date <u>5/23/05</u> </div>
7. Affected Pages	8. Description of Change:
4-4	Deleted a citation Table 4-1 "Direct Inputs for Inclusion of FEPs", page 4-4, 1 st row on page: Delete entire row for entry: LB0311ABSTHCR2.003 [DIRS 166713] This error was identified in CR 4615 Note: This direct input is being removed because it is no longer being used to include the effects of THC processes on seepage chemistry in TSPA.
4-5, 4-6, 4-14, 6-3, 6-4, 6-8, 6-10, 6-11, 6-13, 6-14, 6-16, 6-17, 6-18, 6-19, 6-21, 6-22, 6-23, 6-24, 6-27, 6-28, 6-29, 6-32, 6-33, 6-34, 6-35, 6-36, 6-38, 6-39, 6-40, 6-41, 6-46, 6-47, 6-48, 6-49, 6-50, 6-53, 6-77, 6-94, 6-98, 6-100, 6-101, 6-102, 6-103, 6-104, 6-108, 6-109	Citation update (Correct DIRS as appropriate) Replace Citation, change: BSC 2004 [DIRS 169856] To BSC 2004 [DIRS 172463] This correction is associated with TBV-6598 Additional page 6-40a was added.

Scientific Analysis Administrative Change Notice

Complete only applicable items.

1. Document Number:	ANL-NBS-MD-000001	2. Revision:	03	3. ACN:	01
4. Title:	Features, Events, and Processes in UZ Flow and Transport				
4-8	<p>Deleted a citation</p> <p>Table 4-1 "Direct Inputs for Inclusion of FEPs", page 4-8, 9th row on page:</p> <p>Delete entire row for entry:</p> <p><i>BSC 2004 [DIRS] 170004], Sections 6.2, 6.6</i></p> <p>This error was identified in CR 4615 and is associated with TBV-6601</p>				
4-8	<p>Citation update (Correct DIRS as appropriate)</p> <p>Table 4-1 "Direct Inputs for Inclusion of FEPs", page 4-8, 1st column {Source (in order of DIRS number)}, 18th row on page, change:</p> <p><i>BSC 2004 [DIRS 170007], Section 6.4</i> To <i>BSC 2004 [DIRS 170007], Section 6.6</i></p> <p>This correction is associated with TBV-6607</p>				
4-17	<p>Deleted a citation</p> <p>Table 4-2 "Direct Inputs Used for Exclusion of FEPs", page 4-17, 12th row on page:</p> <p>Delete entire row for entry:</p> <p><i>LB0408RITSSCPF.001 [DIRS 171593]</i></p> <p>This error was identified in CR 4615 and is associated with TBV-6614</p> <p>Note: This direct input is being removed because it is duplicative with the information cited in BSC 2004 [DIRS 169861], Appendix G.</p>				
6-8, 6-10, 6-13, 6-16, 6-18, 6-21, 6-23, 6-27, 6-32, 6-33, 6-35, 6-36, 6-39, 6-41, 6-46, 6-48, 6-49, 6-50	<p>Deleted the following citationon:</p> <p><i>LB0311ABSTHCR2.003 [DIRS 166713]</i></p> <p>This error was identified in CR 4615</p> <p>Additional page 6-33a was added.</p>				

Scientific Analysis Administrative Change Notice

Complete only applicable items.

1. Document Number:	ANL-NBS-MD-000001	2. Revision:	03	3. ACN:	01
4. Title:	Features, Events, and Processes in UZ Flow and Transport				
6-22	<p>Citation update (Correct DIRS as appropriate)</p> <p>Section 6.2.10 "Stratigraphy (2.2.03.01.0A)", TSPA Disposition, 2nd paragraph on page 6-22, 7th line, change:</p> <p><i>BSC 2004 [DIRS 170007], Section 6.4</i> <i>To</i> <i>BSC 2004 [DIRS 170007], Section 6.6</i></p> <p>This correction is associated with TBV-6607</p>				
6-31	<p>Deleted a sentence</p> <p>Section 6.2.18 "Fracture Flow in the UZ (2.2.07.08.0A)", TSPA Disposition, 1st line on page 3-31, delete:</p> <p><i>"These fracture continuum properties are developed from data acquired in In Situ Field Testing of Processes (BSC 2004 [DIRS 170004], Sections 6.2 and 6.6)"</i></p> <p>This correction is associated with TBV-6601</p>				
6-56 and 6-67	<p>Citation update (Correct DIRS as appropriate)</p> <p>Delete the following citation:</p> <p><i>DTN. LB0408RITSSCPF.001 [DIRS 171593]</i></p> <p>This correction is associated with TBV-6614</p>				
6-85	<p>Corrected a value</p> <p>Section 6.8.4 "Hydrologic Response to Igneous Activity (1.2.10.02.0A)", Screening Argument, 4th paragraph, 2nd line, change:</p> <p><i>Bedrock permeability in the infiltration model ranges from 2×10^{-17} to $6 \times 10^{-13} \text{ m}^2$</i> <i>To</i> <i>Bedrock permeability in the infiltration model ranges from 1×10^{-17} to $6 \times 10^{-13} \text{ m}^2$</i></p> <p>This correction is associated with TBV-6607</p>				

Scientific Analysis Administrative Change Notice

Complete only applicable items.

1. Document Number:	ANL-NBS-MD-000001	2. Revision:	03	3. ACN:	01
4. Title:	Features, Events, and Processes in UZ Flow and Transport				
8-3	<p>Citation update (Correct DIRS as appropriate)</p> <p>Section 8.1 "Documents Cited", replace reference (169856) with reference (172463), change:</p> <p><i>BSC 2004. Drift–Scale THC Seepage Model. MDL-NBS-HS-000001, Rev. 03. Las Vegas, Nevada: Bechtel SAIC Company.</i></p> <p>To</p> <p><i>BSC 2004. Drift–Scale THC Seepage Model. MDL-NBS-HS-000001, Rev. 03. Las Vegas, Nevada: Bechtel SAIC Company. ACC: DOC.20041201.0008</i></p> <p>This error was identified in CR 4615 and is associated with TBV-6598</p> <p>Additional page 8-3a was added.</p>				
8-21	<p>Deleted reference (Correct DIRS as appropriate)</p> <p>Deleted the following reference (166713) from section 8.1 "Documents Cited":</p> <p><i>LB0311ABSTHCR2.003. THC Simulations Considering Drift Degradation: Summary/Abstraction Data Files. Submittal date: 11/07/2003</i></p> <p>This error was identified in CR 4615</p>				
8-21	<p>Deleted reference (Correct DIRS as appropriate)</p> <p>Deleted the following reference (1711593) from section 8.1 "Documents Cited":</p> <p><i>LB0408RITSSCPF.001. 3-D Site Scale UZ Flow Simulation for RIT Infiltration Scenario. Submittal date: 08/18/2004.</i></p> <p>This correction is associated with TBV-6614</p>				

Scientific Analysis Administrative Change Notice

Complete only applicable items.

1. Document Number:	ANL-NBS-MD-000001	2. Revision:	03	3. ACN:	01
4. Title:	Features, Events, and Processes in UZ Flow and Transport				
C-6	<p>Corrected Typographical Error</p> <p>Section C6 “Effects of Cementitious Material on Groundwater Quality”, Technical Assessment, DTN: LB0408CMATUZFT.002 [DIRS 172022], line number 13, change:</p> <p><i>“Similar calculations were used to plan carbonation tests over a 1-DTN DTN: LL020711323125.001 [DIRS 172026]”</i></p> <p>To</p> <p><i>“Similar calculations were used to plan carbonation tests over a 100-day period DTN: LL020711323125.001 [DIRS 172026]”</i></p> <p>This error was self identified.</p>				
D-12 and D-13	<p>Added clarification</p> <p>Section D3.1 “Use of SR Model”, 2nd paragraph, line number 14, change:</p> <p><i>"Furthermore, the goal of the present analysis is to compare the relative effects of changes in fracture aperture on UZ transport behavior, and given that the conceptual and numerical models are for the SR and LA models are nearly the same, the SR model should be suitable for assessing transport sensitivity to seismic-induced changes in fracture properties."</i></p> <p>To</p> <p><i>"Furthermore, the goal of the present analysis is to compare the relative effects of changes in fracture aperture on UZ transport behavior. Given that the conceptual and numerical models are for the SR and LA models are nearly the same, the SR model should be suitable for its intended use of assessing transport sensitivity to seismic-induced changes in fracture properties."</i></p> <p>This error was identified in CR 4615</p>				

Table 4-1. Direct Inputs for Inclusion of FEPs (Continued)

Source (in order of DIRS number)	Category	Used in Section Number	Description
LB0311ABSTHCR2.001 [DIRS 166714]	Data	6.2.1, 6.2.2, 6.2.4, 6.2.6, 6.2.7, 6.2.10, 6.2.11, 6.2.13, 6.2.15, 6.2.18, 6.2.19, 6.2.20, 6.2.21, 6.2.26, 6.2.27, 6.2.32, 6.2.34, 6.2.35, 6.2.36	Summary statistics of predicted aqueous species and CO ₂ gas concentrations
LA0311BR831229.001 [DIRS 166924]	Data	6.2.29	Transfer function calculation files for UZ transport abstraction model
LA0311AM831341.001 [DIRS 167015]	Data	6.2.26, 6.2.28, 6.2.30	Correlation matrix for sampling of sorption coefficient probability distributions
BSC 2004 [DIRS 167652], Section 6.3	Data	6.2.2, 6.2.8	Process model of seepage from fractures into drift; treatment of enhanced influx at the repository for drift seepage in TSPA
BSC 2004 [DIRS 167652], Section 6.3.6	Data	6.2.4, 6.2.6, 6.2.7	Climate change and resulting change in percolation flux included in drift seepage model
BSC 2004 [DIRS 167652], Sections 6.3.2, 6.4	Data	6.2.9	Mechanical effects of excavation are included in the seepage model
BSC 2004 [DIRS 167652], Sections 6.3.2, 6.3.3, 6.3.4	Data	6.2.10, 6.2.11	Seepage simulated in Tptpmn and Tptpll layers of TSw
BSC 2004 [DIRS 167652], Sections 6.2.1, 6.3	Data	6.2.13	Conceptual and numerical model of unsaturated groundwater flow used for seepage calculations
BSC 2004 [DIRS 167652], Section 6.8	Data	6.2.15	Treatment of flow focusing in the seepage model
BSC 2004 [DIRS 167652], Sections 6.3.2, 6.3.3	Data	6.2.18	Treatment of fracture flow in the seepage model
BSC 2004 [DIRS 167652], Section 6.3	Data	6.2.19	Matrix imbibition is neglected in the seepage model
BSC 2004 [DIRS 167652], Section 6.3	Data	6.2.23	Film flow is included in the seepage model
BSC 2004 [DIRS 167652], Sections 6.2.1, 6.3.2, 6.7	Data	6.2.25	Flow diversion around opening is included in the seepage model.
BSC 2004 [DIRS 168489]	Data	6.2.1	Heat output from emplaced waste
BSC 2004 [DIRS 169131], Sections 6.4.3.1, 6.5.2	Data	6.2.1	Effect of preclosure ventilation on seepage
BSC 2004 [DIRS 169131], Sections 6.3.1, 6.4, 6.6	Data	6.2.2	Method of deriving seepage-relevant parameters, and probability distributions describing their spatial variability and uncertainty. Abstraction methodology. Effects of THC and THM processes on seepage.

Table 4-1. Direct Inputs for Inclusion of FEPs (Continued)

Source (in order of DIRS number)	Category	Used in Section Number	Description
BSC 2004 [DIRS 169131], Section 6.6.5	Data	6.2.4, 6.2.6, 6.2.7	Percolation flux distributions from flow fields output by UZ flow model
BSC 2004 [DIRS 169131], Section 6.4.1, 6.4.2, 6.4.3	Data	6.2.8	Calculation of ambient seepage, using drift scale model with distributions of seepage-relevant parameters.
BSC 2004 [DIRS 169131], Sections 6.6.2, 6.6.3; Tables 6.6-1 and 6.6-3	Data	6.2.9	Permeability and capillary-strength values, and their probability distributions, for fracture continuum
BSC 2004 [DIRS 169131], Section 6.4	Data	6.2.10	Drift-scale seepage process model.
BSC 2004 [DIRS 169131], Sections 6.4, 6.6.1, 6.6.2, 6.6.5.1	Data	6.2.11	Rock properties used in seepage calculation and seepage abstraction.
BSC 2004 [DIRS 169131], Sections 6.4, 6.6.5.1	Data	6.2.13	Method of calculating seepage. Distribution of values of seepage-relevant parameters. Effects of THC and THM processes on seepage
BSC 2004 [DIRS 169131], Sections 6.4, 6.6.5.2	Data	6.2.15	Flow focusing factor distribution and effect of heterogeneous permeability field
BSC 2004 [DIRS 169131], Sections 6.3.1, 6.4, 6.5.1.4, 6.5.2, 6.6.5, 6.7.1	Data	6.2.18	Inclusion of fracture-flow processes in seepage abstraction.
BSC 2004 [DIRS 169131], Sections 6.4, 6.6.5.1	Data	6.2.19	Matrix imbibition is not included in calculation of seepage from fractures, but is included in calculation of percolation flux.
BSC 2004 [DIRS 169131], Sections 6.3.2, 6.4.3.3, 6.5.2	Data	6.2.20	Inclusion of condensation zone in seepage abstraction.
BSC 2004 [DIRS 169131], Sections 6.4.3, 6.5.2	Data	6.2.21	Inclusion of re-saturation and reflux in seepage abstraction.
BSC 2004 [DIRS 169131], Section 6.4.1.1, Table 6.6-1	Data	6.2.23	Inclusion of film flow in fractures in seepage abstraction.
BSC 2004 [DIRS 169131], Sections 6.4.1, 6.4.2, 6.4.3	Data	6.2.25	Inclusion of flow diversion around drifts, and of drift collapse, in seepage abstraction.
BSC 2004 [DIRS 169131], Sections 6.4.3, 6.4.4	Data	6.2.34	Inclusion of natural geothermal gradient
BSC 2004 [DIRS 169131], Sections 6.3.2, 6.4.3.3, 6.5.2	Data	6.2.35	Inclusion of heat pipe effect
BSC 2004 [DIRS 169131], Sections 6.4.3.3, 6.5.2	Data	6.2.36	Inclusion of geosphere dryout
BSC 2004 [DIRS 169565], Section 5.1.4	Data	6.2.4	Timing of climate change for TSPA
BSC 2004 [DIRS 169855], Entire	Data	6.2.2, 6.2.3, 6.2.10, 6.2.11, 6.2.37	Stratigraphic sequence
BSC 2004 [DIRS 172463], Section 4.1.7, 6.5	Data	6.2.1	Treatment of preclosure ventilation in THC modeling
BSC 2004 [DIRS 172463], Sections 6.2.1, 6.4.3, 6.4.4, 6.4.7	Data	6.2.2, 6.2.18	Treatment of fracture flow in THC modeling

Table 4-1. Direct Inputs for Inclusion of FEPs (Continued)

Source (in order of DIRS number)	Category	Used in Section Number	Description
BSC 2004 [DIRS 172463], Sections 6.2.1.3, 6.5.2	Data	6.2.4, 6.2.6	Treatment of climate change in THC modeling
BSC 2004 [DIRS 172463], Sections 6.2.1, 6.2.1.3, 6.5.2, 6.5.5.2	Data	6.2.7	Percolation flux increases caused by climate change and by contribution of reflux to percolation flux
BSC 2004 [DIRS 172463], Sections 4.1.2, 6.5.1	Data	6.2.10	Treatment of stratigraphy in THC modeling
BSC 2004 [DIRS 172463], Sections 6.4.7, 6.5.5.3, Table 6.4-1	Data	6.2.11	Treatment of rock properties for THC modeling
BSC 2004 [DIRS 172463], Section 6.2.1	Data	6.2.13	Treatment of unsaturated flow and matrix imbibition in THC modeling
BSC 2004 [DIRS 172463], Section 6.3	Data	6.2.15	Treatment of matrix imbibition in THC modeling
BSC 2004 [DIRS 172463], Section 6.2.1; Figure 6.2.3	Data	6.2.19	Treatment of matrix imbibition in THC modeling
BSC 2004 [DIRS 172463], Sections 6.2, 6.5, 6.6	Data	6.2.20	Treatment of condensation in THC modeling
BSC 2004 [DIRS 172463], Sections 6.2.1, 6.5.5	Data	6.2.21	Treatment of resaturation of the rock following dryout in THC modeling
BSC 2004 [DIRS 172463], Sections 6.2.2, 6.5.5; Table 6.2-1	Data	6.2.26	Treatment of variability of groundwater chemistry in THC modeling
BSC 2004 [DIRS 172463], Sections 6.4.4, 6.4.5, 6.5.5.2	Data	6.2.27	Treatment of redissolution of precipitates in THC modeling
BSC 2004 [DIRS 172463], Sections 6.2.1.2, 6.2.2.1, 6.2.2.2	Data	6.2.32	Treatment of THC processes leading to simulation of seepage chemistry
BSC 2004 [DIRS 172463], Section 6.5.2	Data	6.2.34	Treatment of natural geothermal gradient in THC modeling
BSC 2004 [DIRS 172463], Sections 6.2.1.1, 6.2.1.2, 6.5.5.2.2	Data	6.2.35	Treatment of heat pipes and buoyant flow in THC modeling
BSC 2004 [DIRS 172463], Sections 6.2.1, 6.5.5.1	Data	6.2.36	Treatment of geosphere dryout in THC modeling
BSC 2004 [DIRS 172463], Table 6.2-1, Fig. 6.2-4	Data	6.2.40	Treatment of infiltration and recharge in THC modeling
BSC 2004 [DIRS 169857], Section 6.3	Data	6.2.2	Calibration of fracture properties
BSC 2004 [DIRS 169857], Section 6.3.4	Data	6.2.3	Calibration of fault properties
BSC 2004 [DIRS 169857], Section 6.1.4	Data	6.2.10	Treatment of stratigraphy on calibration of flow model
BSC 2004 [DIRS 169857], Section 6.3	Data	6.2.11	Calibration of rock properties
BSC 2004 [DIRS 169857], Section 6.1.4, 6.3.2	Data	6.2.15	Treatment of flow focusing in model calibration, calibration of active-fracture parameter
BSC 2004 [DIRS 169857], Section 6.1.4, 6.3	Data	6.2.13	Calibration of unsaturated flow parameters

Table 4-1. Direct Inputs for Inclusion of FEPs (Continued)

Source (in order of DIRS number)	Category	Used in Section Number	Description
BSC 2004 [DIRS 169861], Sections 6.1.3, 6.1.4	Data	6.2.38	Treatment of precipitation through the infiltration model in the UZ flow model
BSC 2004 [DIRS 169861], Sections 6.1.3, 6.1.4	Data	6.2.39	Treatment of surface runoff and flooding through the infiltration model in the UZ flow model
BSC 2004 [DIRS 169861], Section 6.1.4	Data	6.2.40	Treatment of infiltration and recharge in the UZ flow model
BSC 2004 [DIRS 170002], Section 6.6	Data	6.2.4	Treatment of climate change
BSC 2004 [DIRS 170004], Section 6.1, 6.2	Data	6.2.2, 6.2.13	Data used to derive seepage-relevant parameters
BSC 2004 [DIRS 170004], Section 6.6	Data	6.2.2	Data describing fracture-matrix interaction
BSC 2004 [DIRS 170004], Section 6.1	Data	6.2.9	Measurements that include the effects of construction
BSC 2004 [DIRS 170004], Sections 6.1, 6.2	Data	6.2.13	Data describing unsaturated flow
BSC 2004 [DIRS 170004], Section 6.4	Data	6.2.19	Data from matrix imbibition tests
BSC 2004 [DIRS 170004], Section 6.2	Data	6.2.23, 6.2.25	Measurements that demonstrate flow diversion around niches and include the effects of film flow into niches
BSC 2004 [DIRS 170004], Section 6.12	Data	6.2.40	Infiltration test data
BSC 2004 [DIRS 170006], Section 6.4.3	Data	6.2.31	Colloid retardation factors
BSC 2004 [DIRS 170007], Section 6.1, Appendix B	Data	6.2.2	Treatment of fractures in infiltration model
BSC 2004 [DIRS 170007], Section 6.9	Data	6.2.4	Inclusion of future climate states in infiltration model
BSC 2004 [DIRS 170007], Section 6.3.4	Data	6.2.12	Treatment of saturated flow at bedrock/alluvium contact in infiltration model
BSC 2004 [DIRS 170007], Section 6.11	Data	6.2.6, 6.2.7	Percolation flux and increased percolation due to climate change in infiltration model
BSC 2004 [DIRS 170007], Section 6.6	Data	6.2.10	Treatment of stratigraphy in infiltration model
BSC 2004 [DIRS 170007], Section 6.6.4, Appendix B	Data	6.2.11	Treatment of rock properties in infiltration model
BSC 2004 [DIRS 170007], Sections 6.1.2, 6.11	Data	6.2.13	Treatment of unsaturated flow in infiltration model
BSC 2004 [DIRS 170007], Sections 6.1.2, 6.3.4	Data	6.2.18	Treatment of fracture flow in infiltration model
BSC 2004 [DIRS 170007], Sections 6.5.3, 6.6.1, Appendix D	Data	6.2.37	Treatment of topography and morphology in infiltration model
BSC 2004 [DIRS 170007], Sections 6.4, 6.9	Data	6.2.38	Treatment of precipitation in infiltration model
BSC 2004 [DIRS 170007], Section 6.4	Data	6.2.39	Treatment of surface runoff and flooding in infiltration model

Table 4-2. Direct Inputs Used for Exclusion of FEPs (Continued)

Source (in order of DIRS number)	Type	Used in Section Number	Description
BSC 2004 [DIRS 169131], Section 6.5.1.4	Data	6.9.1, 6.9.10	Effects of temperature-induced stress changes on permeability
BSC 2004 [DIRS 169131], Sections 6.4.4.1.2, 6.5.1.5	Data	6.8.6	Effects of drift collapse on seepage-relevant hydrologic properties.
BSC 2004 [DIRS 169425], Section 6.3.3.3	Data	6.9.8	Solubility of actinides at elevated temperature
LB0306DRSCLTHM.001 [DIRS 169733]	Data	6.5.4	Subsidence calculations for drifts
BSC 2004 [DIRS 169734], Section 6.4.1.4	Data	6.4.2	Information on glaciation near Yucca Mountain
BSC 2004 [DIRS 169734], Section 3.3.2	Data	6.5.3	Bulk mineral composition of Yucca Mountain
BSC 2004 [DIRS 169734], Section 4.2.3.5	Data	6.8.2, 6.8.4	Spatial extent of contact metamorphism
BSC 2004 [DIRS 169734], Section 3.6.2	Data	6.8.2	Evidence for hydrothermal activity
BSC 2004 [DIRS 169855], Section 5.2	Data	6.9.16	Location of zeolites in the UZ
BSC 2004 [DIRS 169855], Figures 6-6 through 6-8	Data	6.9.16	Location of zeolites in the UZ
BSC 2004 [DIRS 172463], Section 6.5.5.3	Data	6.9.1, 6.9.7, 6.9.13	Changes in fracture permeability due to THC processes
BSC 2004 [DIRS 172463], Figures 6.5-39 and 6.5-40	Data	6.9.1, 6.9.7, 6.9.13	Changes in fracture permeability due to THC processes
BSC 2004 [DIRS 172463]	Data	6.9.7	Effects of THC processes on water composition
BSC 2004 [DIRS 172463], Figures 6.5-12, 6.5-25, 6.5-58	Data	6.9.7, 6.9.13	Effects of THC processes on pH
BSC 2004 [DIRS 172463], Table 6.2-1	Data	6.9.7, 6.9.13	Range of variability in pH for porewater compositions
BSC 2004 [DIRS 172463], Figure 6.5-16	Data	6.9.7, 6.9.13	Effects of THC processes on water aqueous silica, Ca, Na, and Cl
BSC 2004 [DIRS 169860], Table 6.6-4	Data	6.9.2	Seepage water composition
BSC 2004 [DIRS 169860], Tables 6.6-8 through 6.6-12	Data	6.9.2	Seepage water composition
BSC 2004 [DIRS 169860], Section 6.8	Data	6.9.2	Effects of stainless steel on water composition
BSC 2004 [DIRS 169860], Section 6.12.4.1	Data	6.9.2	Effects of stainless steel on water composition
BSC 2004 [DIRS 169860], Section 6.12.4.1.3	Data	6.9.2	Effects of stainless steel on water composition
BSC 2004 [DIRS 169861], Figure H-2	Data	6.3.6, 6.3.7, 6.3.8	Breakthrough curve at repository horizon for ³⁶ Cl infiltrating at surface
BSC 2004 [DIRS 169861] Appendix G	Data	6.4.5	Damping effect of PTn on episodic infiltration

Table 4-2. Direct Inputs Used for Exclusion of FEPs (Continued)

Source (in order of DIRS number)	Type	Used in Section Number	Description
BSC 2004 [DIRS 170038], Table 6-5	Data	6.3.1, 6.9.7, 6.9.13	Fracture area per unit volume
BSC 2004 [DIRS 170040], Table E-2	Data	6.9.17	Effects of fracture aperture on fracture-matrix partitioning of radionuclides entering the UZ
BSC 2004 [DIRS 170041], Section 6.4.5	Data	6.9.13	Treatment of colloid-facilitated transport
BSC 2004 [DIRS 170041], Tables 6-2 and 6-13	Data	6.9.17	Values for dispersivity and fracture porosity
BSC 2004 [DIRS 170041], Table 6-6	Data	6.8.8	Minimum average water content of rock in the UZ within 100 m of the water table.
BSC 2004 [DIRS 170058]	Data	6.9.2	Use of cementitious materials for ground support
BSC 2004 [DIRS 170338], Section 6.2.2.1	Data	6.9.9	Diversion of water around thermal dryout zone
BSC 2004 [DIRS 170338], Section 6.2.1.3.3	Data	6.9.4	Effects of preclosure dryout on thermal seepage
BSC 2004 [DIRS 170338], Section 6.2.2.1.1	Data	6.9.9	Effects of thermal dryout and drift shadow on radionuclide transport
BSC 2004 [DIRS 170505], Sections 3.3.1.4, 3.3.2	Data	6.3.5	Effects of monitoring activities on repository performance
LB0308DRSCLTHM.001 [DIRS 171567]	Data	6.5.4	Subsidence calculations for drift in Tptll low-quality rock
BSC 2004 [DIRS 171676], Sections 3.1.1.13.1 through 3.1.1.13.3	Data	6.3.3, 6.3.7, 6.3.8	Design requirement concerning surface water inundation of the subsurface facilities
LB0408CMATUZFT.004 [DIRS 171706]	Data qualified in accordance with AP-SIII.2Q; see Appendix C, Section C6	6.9.2	Diffusion and dispersion of plumes of leachate from altered cementitious materials.
LB0408CMATUZFT.003 [DIRS 171705]	Data qualified in accordance with AP-SIII.2Q; see Appendix C, Section C6	6.9.2	Chemistry of leachate from altered cementitious materials

LA = license application; TH = thermal hydrologic; THC = thermal-hydrologic-chemical; THM = thermal-hydrologic-mechanical; TSPA = total system performance assessment; UZ = unsaturated zone.

system that contribute to performance are not amplified by changes in UZ performance. The performance of the waste package outer barrier and drip shield over 10,000 years depends on temperature, relative humidity, and water chemistry derived from seepage water chemistry, but is not a strong function of drift seepage quantity (BSC 2004 [DIRS 169984], Figure 6-1; BSC 2004 [DIRS 169845], Figure 1). Seepage water chemistry is determined mainly by water–rock interaction and evaporative concentration in the near-field, and the uncertainty in seepage water chemistry determined by the uncertainty in initial water chemistry, as discussed in *Drift-Scale THC Seepage Model* (BSC 2004 [DIRS 172463]), Section 6.6.2). Also, the rate of radionuclide transport in the saturated zone is independent of the source-term strength. Therefore, some FEPs may have a significant effect on radionuclide transport or drift seepage in the UZ and yet have an insignificant effect on total system performance, because of the contributions of the other system components to total system performance. Thus, if a FEP can be shown to have minimal consequence on the UZ subsystem performance, and is not included by any other FEP report, then it will also have a minimal consequence on total system performance in terms of the time or magnitude of the resulting radiological exposures to the reasonably maximally exposed individual, or radionuclide releases to the accessible environment. The rationale for exclusion is given in the screening argument presented for each excluded FEP. Sections 6.3 through 6.9 discuss FEPs that are excluded from TSPA-LA.

The following standardized format is used to present the status of each FEP as presented in the third-order subsections of this chapter. Documentation of the screening for each FEP is provided in Sections 6.2 through 6.9. The following standardized format is used.

Third-Order Subsection Heading: FEP Name (FEP Number)

FEP Description: This field describes the nature and scope of the FEP under consideration.

Screening Decision: Identifies the screening decision as one of:

- “Included”
- “Excluded–Low Probability”
- “Excluded–Low Consequence”
- “Excluded–By Regulation.”

A few FEPs are excluded by a combination of two criteria (e.g., Low Probability and Low Consequence).

Screening Argument: This field is used only for excluded FEPs. It provides the discussion for why a FEP has been excluded from TSPA-LA.

TSPA Disposition: This field is used only for included FEPs. It provides the consolidated discussion of how a FEP has been included in TSPA-LA, making reference to more detailed documentation in other supporting technical reports, as applicable.

Supporting Reports: This field is only used for included FEPs. It provides the list of supporting technical reports that identified the FEP as an included FEP and contain information relevant to the implementation of the FEP within the TSPA-LA model. This list of supporting

technical reports provides traceability of the FEP through the document hierarchy. For excluded FEPs, it is indicated as “Not applicable.”

6.1.3 Supporting Reports and Inputs

For included FEPs, the model reports develop the models or parameters. These are passed to abstraction reports and then to the TSPA model. In some cases, process model reports pass outputs directly to the TSPA model (e.g., in the flow fields that are output from *UZ Flow Models and Submodels* [BSC 2004 (DIRS 169861)]). Reports that discuss the subject matter of a FEP, but do not develop any input that is eventually used in, or abstracted for use in, the TSPA model are not listed as supporting reports in the disposition of included FEPs. Supporting reports are listed below.

- *Abstraction of Drift Seepage* (BSC 2004 [DIRS 169131])
- *Analysis of Hydrologic Properties Data* (BSC 2004 [DIRS 170038])
- *Analysis of Infiltration Uncertainty* (BSC 2004 [DIRS 165991])
- *Calibrated Properties Model* (BSC 2004 [DIRS 169857])
- *Conceptual Model and Numerical Approaches for UZ Flow and Transport* (BSC 2004 [DIRS 170035])
- *Development of Numerical Grids for UZ Flow and Transport Modeling* (BSC 2004 [DIRS 169855])
- *Drift Scale THM Model* (BSC 2004 [DIRS 169864])
- *Drift-Scale Coupled Processes (DST and TH Seepage) Models* (BSC 2004 [DIRS 170338])
- *Drift-Scale THC Seepage Model* (BSC 2004 [DIRS 172463])
- *Future Climate Analysis* (BSC 2004 [DIRS 170002])
- *In Situ Field Testing of Processes* (BSC 2004 [DIRS 170004])
- *Mountain-Scale Coupled Processes (TH/THC/THM)* (BSC 2004 [DIRS 169866])
- *Particle Tracking Model and Abstraction of Transport Processes* (BSC 2004 [DIRS 170041])
- *Post-Processing Analysis for THC Seepage* (BSC 2004 [DIRS 169858])
- *Radionuclide Transport Models Under Ambient Conditions* (BSC 2004 [DIRS 164500])

[DIRS 169131], Section 6.5.2). The effects of preclosure ventilation on dryout of the rock are the same for the THC model as for the TH model.

The effect of preclosure ventilation on the thermal load provided to the rock is also explicitly simulated with the THC seepage model that feeds into the drift-scale coupled processes abstraction model, by using time-dependent boundary conditions for the thermal load (BSC 2004 [DIRS 172463], Sections 4.1.7 and 6.5). These boundary conditions reflect the current emplacement design (waste package spacing, average heat output of waste canisters, etc.), provided in the design drawings (BSC 2004 [DIRS 168489]).

The results from the THC seepage model, and their abstraction (BSC 2004 [DIRS 169858], Section 6.2), account for the impact of preclosure ventilation and waste package spacing on the THC conditions in the near-drift rock. Summary tables of concentrations through time are presented in DTNs: LB0302DSCPTHCS.002 [DIRS 161976]; LB0307DSTTHCR2.002 [DIRS 165541], and summary statistics through time are presented in LB0311ABSTHCR2.001 [DIRS 166714]. These data are used to feed and/or provide technical basis for *Engineered Barrier System: Physical and Chemical Environment Model* (BSC 2004 [DIRS 169860]), which generates look-up tables used in the TSPA-LA model.

Supporting Reports: *Abstraction of Drift Seepage* (BSC 2004 [DIRS 169131]); *Drift-Scale THC Seepage Model* (BSC 2004 [DIRS 172463]); *Drift-Scale Coupled Processes (DST and TH Seepage) Models* (BSC 2004 [DIRS 170338]).

6.2.2 Fractures (1.2.02.01.0A)

FEP Description: Groundwater flow in the Yucca Mountain region and transport of any released radionuclides may take place along fractures. The rate of flow and the extent of transport in fractures are influenced by characteristics such as orientation, aperture, asperity, fracture length, connectivity, and the nature of any linings or infills.

Screening Decision: Included.

TSPA Disposition: This FEP on “Fractures” is included in process models for UZ flow and transport. The UZ flow model is based on a dual-permeability concept, with fractures and matrix each represented by a continuum in the dual permeability mesh (BSC 2004 [DIRS 169855]). The fracture continuum represents the spatially averaged flow through discrete fractures. The fracture continuum interacts with the matrix continuum, which represents matrix blocks separated by fractures.

Fracture continuum properties include permeability, porosity, interface area per unit volume, van Genuchten α and m parameters for the saturation-capillary pressure and relative permeability functions, and an active fracture parameter. These parameters and associated range of values are obtained as described in *UZ Flow Models and Submodels* (BSC 2004 [DIRS 169861], Section 6.1.5) and adjusted as described in *UZ Flow Models and Submodels* (BSC 2004 [DIRS 169861], Section 6.2.3) for each UZ model layer (DTN: LB0205REVUZPRP.001 [DIRS 159525] and LB0209DSSCFPR.002 [DIRS 162128]).

conducted within the TSPA-LA by sampling from these probability distributions and interpolating seepage rates from the look-up tables given in DTNs: LB0304SMDCREV2.002 [DIRS 163687] and LB0307SEEPDRCL.002 [DIRS 164337]. During the thermal period, the ambient seepage rates will be adjusted based on the TH-modeling results from *Drift-Scale Coupled Processes (DST and TH Seepage) Models* (BSC 2004 [DIRS 170338]), which explicitly simulates the thermally perturbed fracture flow conditions. Results are given in DTN: LB0301DSCPTHSM.002 [DIRS 163689]. THM and THC effects on fracture characteristics are evaluated with process models that explicitly account for fracture flow affected by THM and THC parameter alterations (BSC 2004 [DIRS 169131], Section 6.4.4; see FEPs 2.1.09.12.0A and 2.2.10.04.0A). It was demonstrated that these potential alterations can be neglected in the TSPA-LA, because the expected changes would lead to less seepage (BSC 2004 [DIRS 169131], Section 6.5.1.4), and therefore would result in predictions that underestimate repository performance.

Flow processes in fractures or other channels affect modeled THC coupled processes because of (1) their strong effect on TH behavior (BSC 2004 [DIRS 169131], Sections 6.4.4.1 and 6.4.4.2), and (2) their strong effect on water and gas chemistry (BSC 2004 [DIRS 172463], Section 6.2.1). The latter is primarily due to volatilization of steam and CO₂ from the rock matrix-water and subsequent transport and condensation in fractures. The amount of mobilized CO₂ with steam directly affects the pH of the condensate, which in turn affects the degree of water-rock interaction and water chemistry. These THC processes are influenced by the fracture characteristics, such as orientation, aperture, asperity, length, connectivity, and fillings. The THC seepage model that feeds into the drift scale coupled processes abstraction model explicitly simulates the flow processes in fractures using appropriate continuum properties that represent these characteristics (BSC 2004 [DIRS 172463], Sections 6.4.3, 6.4.4, and 6.4.7).

Thus, the results from the THC seepage model and their abstraction (BSC 2004 [DIRS 169858], Section 6.2), and tables of concentrations and summary statistics through time, implicitly account for the effect of climate change on THC processes. Summary tables of concentrations through time are presented in DTNs: LB0302DSCPTHCS.002 [DIRS 161976]; LB0307DSTTHCR2.002 [DIRS 165541]; and summary statistics through time are presented in LB0311ABSTHCR2.001 [DIRS 166714]. These data are used to feed and/or provide technical basis for *Engineered Barrier System: Physical and Chemical Environment Model* (BSC 2004 [DIRS 169860]), which generates look-up tables used in the TSPA-LA model.

The effects of fractures are also included in the treatment of infiltration uncertainty for TSPA-LA (BSC 2003 [DIRS 165991]). Infiltration uncertainty is represented through three discrete infiltration scenarios (lower, mean, and upper), which are sampled in TSPA-LA according to weighting factors (BSC 2003 [DIRS 165991], Section 7.1). Fractures are included in the infiltration uncertainty analysis by incorporation of the fracture parameters for bedrock permeability (BRPERM) and bedrock porosity (BRPOROS) that are included implicitly in the determination of the weighting factors. *Analysis of Infiltration Uncertainty* (BSC 2003 [DIRS 165991], Table 6-1) defines these fracture parameters and their uncertainties (BSC (2003 [DIRS 165991], Tables 6-2 and 6-3). These uncertainties are propagated through the infiltration numerical model and so are implicitly included in the output (weighting factors)

that is passed to TSPA-LA (BSC 2003 [DIRS 165991]; DTN: SN0308T0503100.008 [DIRS 165640]).

Supporting Reports: *Simulation of Net Infiltration for Present-Day and Potential Future Climates* (BSC 2004 [DIRS 170007]); *Development of Numerical Grids for UZ Flow and Transport Modeling* (BSC 2004 [DIRS 169855]); *In Situ Field Testing of Processes* (BSC 2004 [DIRS 170004]); *Calibrated Properties Model* (BSC 2004 [DIRS 169857]); *UZ Flow Models and Submodels* (BSC 2004 [DIRS 169861]); *Particle Tracking Model and Abstraction of Transport Processes* (BSC 2004 [DIRS 170041]); *Seepage Model for PA Including Drift Collapse* (BSC 2004 [DIRS 167652]); *Seepage Calibration Model and Seepage Testing Data* (BSC 2004 [DIRS 171764]); *Analysis of Hydrologic Properties Data* (BSC 2004 [DIRS 170038]), *Drift-Scale THC Seepage Model* (BSC 2004 [DIRS 172463]), *Abstraction of Drift Seepage* (BSC 2004 [DIRS 169131]), *Drift-Scale Coupled Processes (DST and TH Seepage) Models* (BSC 2004 [DIRS 170338]), *Analysis of Infiltration Uncertainty* (BSC 2003 [DIRS 165991]).

6.2.3 Faults (1.2.02.02.0A)

FEP Description: Numerous faults of various sizes have been noted in the Yucca Mountain region and specifically in the repository area. Faults may represent an alteration of the rock permeability and continuity of the rock mass, an alteration or short-circuiting of the flow paths and flow distributions close to the repository, and/or unexpected pathways through the repository.

Screening Decision: Included

TSPA Disposition: The stratigraphic units/layers and fault geometries are defined in *Geological Framework Model (GFM2000)* (BSC 2004 [DIRS 170029]) and DTN: MO0012MWDGFM02.002 [DIRS 153777]). This provides the basis the UZ model grid in *Development of Numerical Grids for UZ Flow and Transport Modeling* (BSC 2004 [DIRS 169855]). Major displacement, dip-slip, strike-slip, and detachment faults within the model domain are explicitly discretized in the mountain-scale UZ flow and transport models described in *UZ Flow Models and Submodels* (BSC 2004 [DIRS 169861], Sections 6.1.5, 6.2.2, 6.6.3, 6.7.3) and *Development of Numerical Grids for UZ Flow and Transport Modeling* (BSC 2004 [DIRS 169855], Sections 6.4 and 6.6.1). These faults are represented in the UZ model grid developed in *Development of Numerical Grids for UZ Flow and Transport Modeling* (BSC 2004 [DIRS 169855]) as vertical or inclined discrete zones 30 m wide, and include existing displacements that affect the relative geometry of the hydrogeologic model units. Specific hydrogeologic properties are assigned to the fault zones. Fault properties (matrix and fracture parameters) are in DTN: LB02092DSSCFPR.002 [DIRS 162128] and in *UZ Flow Models and Submodels* (BSC 2004 [DIRS 169861], Table 4.1-1). These properties have been calibrated as described in *Calibrated Properties Model* (BSC 2004 [DIRS 169857], Section 6.3.4) and *Analysis of Hydrologic Properties Data* (BSC 2004 [DIRS 170038]). The fault properties are used as inputs to the UZ flow model, and their effects are incorporated into the output flow fields developed for use in TSPA-LA (output flow fields are in DTN: LB0305TSPA18FF.001 [DIRS 165625]).

Future climate conditions are addressed in the infiltration model (BSC 2004 [DIRS 170007], Section 6.9) through the selection of analogues at other locations with present day climates that are representative of the range of future climate conditions at Yucca Mountain (BSC 2004 [DIRS 170002], Section 6.6). The meteorological data from these analogues are then used for modeling infiltration under future climate conditions at Yucca Mountain. A description of the modeling methods used for infiltration, and of how infiltration is affected by climate, is given in *Simulation of Net Infiltration for Present-Day and Potential Future Climates* (BSC 2004 [DIRS 170007], Section 6.9). The results of the infiltration model are then used for computing UZ flow throughout the UZ flow-model domain, which includes the repository waste emplacement zone. The UZ flow model uses the infiltration results as top boundary conditions for UZ flow calculations (BSC 2004 [DIRS 169861], Section 6.1.4). The UZ flow fields are used directly in TSPA-LA (BSC 2004 [DIRS 169861], Section 6.2.5). The output flow fields are in DTN: LB0305TSPA18FF.001 [DIRS 165625], developed for use in Performance Assessment (BSC 2003 [DIRS 166296]); the conversion of flow fields to the format needed for use in TSPA is documented in *UZ Flow Models and Submodels* (BSC 2004 [DIRS 169861], Appendix D).

Climate change is implicitly included in the treatment of radionuclide transport for TSPA-LA as discussed in *Particle Tracking Model and Abstraction of Transport Processes* (BSC 2004 [DIRS 170041], Section 6.4.8). The effect of climate change on repository performance was studied by using pregenerated flow fields under different climates (DTN: LB0305TSPA18FF.001 [DIRS 165625]). For TSPA-LA, the pregenerated flow fields are used by the FEHM model as described in *Particle Tracking Model and Abstraction of Transport Processes* (BSC 2004 [DIRS 170041], Section 6.4.9). *Particle Tracking Model and Abstraction of Transport Processes* (BSC 2004 [DIRS 170041]) transmits software and parameters, which incorporate climate change through the flow fields for use in TSPA-LA, but does not generate a direct data feed to TSPA-LA pertaining to this FEP.

Potential effects of climate change on the amount of infiltration and percolation at Yucca Mountain are taken implicitly into account in the THC seepage model by considering different climate stages and climate scenarios when setting infiltration rates at the top model boundary (BSC 2004 [DIRS 172463], Sections 6.2.1.3 and 6.5.2). Thus, the results from the THC seepage model and their abstraction (BSC 2004 [DIRS 169858], Section 6.2), and tables of concentrations and summary statistics through time, implicitly account for the effect of climate change on THC processes. Summary tables of concentrations through time are presented in DTNs: LB0302DSCPTHCS.002 [DIRS 161976], LB0307DSTTHCR2.002 [DIRS 165541], and summary statistics through time are presented in LB0311ABSTHCR2.001 [DIRS 166714]. These data are used to feed and/or provide technical basis for *Engineered Barrier System: Physical and Chemical Environment Model* (BSC 2004 [DIRS 169860]), which generates look-up tables used in the TSPA-LA model. Note that seepage is calculated in the TSPA-LA using percolation flux distributions based on results from the UZ flow and transport model (BSC 2004 [DIRS 169131], Section 6.6.5.1), given in DTNs: LB0302PTNTSW9I.001 [DIRS 162277] and LB0305PTNTSW9I.001 [DIRS 163690]. These flux distributions are based on the same varying climate stages and scenarios identified and used in the THC seepage model.

Potential effects of climate change on the amount of infiltration and percolation at Yucca Mountain are taken into account in the seepage abstraction by considering different climate

stages and climate scenarios in *Abstraction of Drift Seepage* (BSC 2004 [DIRS 169131], Section 6.6.5; and in *Drift-Scale Coupled Processes (DST and TH Seepage) Models* (BSC 2004 [DIRS 170338], Section 6.2). Seepage is calculated in the TSPA-LA using percolation flux distributions based on results from the UZ flow and transport model (BSC 2004 [DIRS 169131], Section 6.6.5.1), given in DTNs: LB0302PTNTSW9I.001 [DIRS 162277] and LB0305PTNTSW9I.001 [DIRS 163690]. These flux distributions include different climate stages and scenarios.

The effects of climate change are also included in the treatment of infiltration uncertainty for TSPA-LA (BSC 2003 [DIRS 165991]). Infiltration uncertainty is represented through three discrete infiltration scenarios (lower, mean, and upper), which are sampled in TSPA-LA according to weighting factors (BSC 2003 [DIRS 165991], Section 7.1). Climate change is incorporated through the use of the analogue climate (lower-bound, mean, and upper-bound) infiltration rate maps (BSC 2003 [DIRS 165991], Table 6-7; DTN: GS000308311221.005 [DIRS 147613]) developed in *Simulation of Net Infiltration for Present-Day and Potential Future Climates* (BSC 2004 [DIRS 170007]) by using the climate analogue data as direct input. It is incorporated implicitly by inclusion of the spatial average analogue net infiltration rate maps in the calculation of the weighting factors passed to TSPA-LA (BSC 2003 [DIRS 165991]; DTN: SN0308T0503100.008 [DIRS 165640]).

The effects of climate change are also included in the treatment of seepage in *Seepage Model for PA Including Drift Collapse* (BSC 2004 [DIRS 167652], Section 6.3.6) and *Drift-Scale Coupled Processes (DST and TH Seepage) Models* (BSC 2004 [DIRS 170338]) through the use of percolation fluxes taken from flow fields calculated for present and future climate states; and in *Drift-Scale Coupled Processes (DST and TH Seepage) Models* (BSC 2004 [DIRS 170338]) through the use of varying flux boundary conditions applied at the top of the model.

Supporting Reports: *Future Climate Analysis* (BSC 2004 [DIRS 170002]); *Simulation of Net Infiltration for Present-Day and Potential Future Climates* (BSC 2004 [DIRS 170007]); *UZ Flow Models and Submodels* (BSC 2004 [DIRS 169861]); *Abstraction of Drift Seepage* (BSC 2004 [DIRS 169131]); *Drift-Scale Coupled Processes (DST and TH Seepage) Models* (BSC 2004 [DIRS 170338]); *Particle Tracking Model and Abstraction of Transport Processes* (BSC 2004 [DIRS 170041]); *Seepage Model for PA Including Drift Collapse* (BSC 2004 [DIRS 167652]); *Drift-Scale THC Seepage Model* (BSC 2004 [DIRS 172463]); *Analysis of Infiltration Uncertainty*, (BSC 2003 [DIRS 165991]).

6.2.5 Water Table Rise Affects UZ (1.3.07.02.0B)

FEP Description: Climate change could produce increased infiltration, leading to a rise in the regional water table, possibly affecting radionuclide release from the repository by altering flow and transport pathways in the UZ. A regionally higher water table and change in UZ flow patterns might flood the repository.

Screening Decision: Included.

TSPA Disposition: The water table will be higher in future climates with greater infiltration (see Table 6-2). To include this water table rise in TSPA-LA calculations, the water table elevation is

Infiltration for Present-Day and Potential Future Climates (BSC 2004 [DIRS 170007], Section 6.11). The nine base-case flow fields and nine alternative flow fields are presented in *UZ Flow Models and Submodels* (BSC 2004 [DIRS 169861], Section 6.6). The output flow fields are in DTN: LB0305TSPA18FF.001 [DIRS 165625], developed for use in performance assessment (BSC 2003 [DIRS 166296]); the conversion of flow fields to the format needed for use in TSPA is documented in *UZ Flow Models and Submodels* (BSC 2004 [DIRS 169861], Appendix D).

Above the repository, perched water bodies were neither observed in the field nor predicted by the UZ flow model. The potential effect of perched water above the repository is indirectly related to lateral diversion of percolation flux in the PTn above the repository. PTn effects on the flow field are discussed in *UZ Flow Models and Submodels* (BSC 2004 [DIRS 169861], Section 6.6). The potential for water table rise caused by climate change is included in TSPA-LA calculations by adjusting the flow fields to the higher water tables (implemented by software WTRISE (LBNL 2003 [DIRS 163453])).

The effect of climate changes in the form of increased recharge is implicitly included in the transport model for TSPA-LA through the use of pregenerated flow fields (BSC 2004 [DIRS 170041], Section 6.5.1 and DTN: LB0305TSPA18FF.001 [DIRS 165625]). In multirealization TSPA-LA runs, different climate patterns are applied and the effect of climate change is included through FEHM's use of pregenerated flow fields for the corresponding climates as described in *Particle Tracking Model and Abstraction of Transport Processes* (BSC 2004 [DIRS 170041], Section 6.5.1). *Particle Tracking Model and Abstraction of Transport Processes* (BSC 2004 [DIRS 170041]) provides a model for use in TSPA-LA, but does not generate a direct data feed to TSPA-LA pertaining to this FEP.

Potential effects of climate change on the amount of infiltration and percolation at Yucca Mountain are taken into account in the THC seepage model by implicitly considering different climate stages and climate scenarios when setting infiltration rates at the top model boundary (BSC 2004 [DIRS 172463], Sections 6.2.1.3 and 6.5.2).

Thus, the results from the THC seepage model, and their abstraction in *Post-Processing Analysis for THC Seepage* (BSC 2004 [DIRS 169858], Section 6.2), implicitly account for the effect of climate change on predicted water and gas chemistry. Summary tables of concentrations through time are presented in DTNs: LB0302DSCPTHCS.002 [DIRS 161976], LB0307DSTTHCR2.002 [DIRS 165541], and summary statistics through time are presented in LB0311ABSTHCR2.001 [DIRS 166714]. These data are used to feed and/or provide technical basis for *Engineered Barrier System: Physical and Chemical Environment Model* (BSC 2004 [DIRS 169860]), which generates lookup tables used in the TSPA-LA model. Potential effects of climate change on the amount of flux through the repository are taken into account in the seepage modeling and abstraction by considering different climate stages and climate scenarios (BSC 2004 [DIRS 169131], Section 6.6.5). The method for calculating seepage in the TSPA-LA (BSC 2004 [DIRS 167652], Section 6.3.6); BSC 2004 [DIRS 170338]; BSC 2004 [DIRS 169131], Section 6.6.5.1) uses percolation flux distributions based on results from *UZ Flow Model and Submodels* (BSC 2004 [DIRS 169861]), given in DTNs: LB0302PTNTSW9I.001 [DIRS 162277] and LB0305PTNTSW9I.001 [DIRS 163690]. These flux distributions are based on the same varying climate stages and scenarios as identified and used in the THC seepage model.

Supporting Reports: *UZ Flow Models and Submodels* (BSC 2004 [DIRS 169861]); *Seepage Model for PA Including Drift Collapse* (BSC 2004 [DIRS 167652]); *Drift-Scale THC Seepage Model* (BSC 2004 [DIRS 172463]); *Abstraction of Drift Seepage* (BSC 2004 [DIRS 169131]); *Drift-Scale Coupled Processes (DST and TH Seepage) Models* (BSC 2004 [DIRS 170338]); *Simulation of Net Infiltration for Present-Day and Potential Future Climates* (BSC 2004 [DIRS 170007]); *Particle Tracking Model and Abstraction of Transport Processes* (BSC 2004 [DIRS 170041]).

6.2.7 Water Influx at the Repository (2.1.08.01.0A)

FEP Description: An increase in the unsaturated water flux at the repository may affect thermal, hydrologic, chemical, and mechanical behavior of the system. Increases in flux could result from climate change, but the cause of the increase is not an essential part of the FEP.

Screening Decision: Included.

TSPA Disposition: This FEP is considered to be included implicitly in the TSPA-LA. Changes in UZ flow in response to climate changes are incorporated in the infiltration maps developed in *Simulation of Net Infiltration for Present-Day and Future Climates* (BSC 2004 [DIRS 170007], Section 6.11) and in output flow fields developed for use in the TSPA-LA by *UZ Flow Models and Submodels* (BSC 2004 [DIRS 169861], Section 6.6.3); the output flow fields are in DTN: LB0305TSPA18FF.001 [DIRS 165625]). Furthermore, the outputs from *UZ Flow Models and Submodels* (BSC 2004 [DIRS 169861]) are also used by other models and evaluations that are intermediate between the UZ flow model and the TSPA-LA model. For example, the flow fields are used to calculate seepage flux in *Seepage Model for PA Including Drift Collapse* (BSC 2004 [DIRS 167652], Section 6.3.6) and *Abstraction of Drift Seepage* (BSC 2004 [DIRS 169131]).

In TSPA-LA multirealization runs, climate changes and the change of water influx at the repository on radionuclide transport are addressed through the use of corresponding pregenerated flow fields. Release of tracked particles (the transport modeling method used for TSPA-LA) is related to the percolation flux at the repository as described in *Particle Tracking Model and Abstraction of Transport Processes* (BSC 2004 [DIRS 170041], Section 6.5.15).

The thermal model output from *UZ Flow Models and Submodels* (BSC 2004 [DIRS 169861]) is used for setting initial conditions for the downstream mountain-scale coupled process evaluation. The effects of changes in UZ flow caused by climate change are also included in the calculations for the thermal-hydrologic (TH) behavior of the repository system in *Mountain-Scale Coupled Processes (TH/THC/THM)* (BSC 2004 [DIRS 169866], Section 6); however, the results are not implemented in TSPA because they are used only to support arguments for the exclusion of certain FEPs. The effects of transient flow driven by thermal-hydrologic processes are also included in TSPA-LA calculations for drift seepage in *Abstraction of Drift Seepage* (BSC 2004 [DIRS 169131]). The effects of THC and THM on seepage are also addressed in the seepage abstraction report.

The potential increase in the magnitude of percolation flux at the repository, as a result of climate changes or flow focusing effects, is accounted for in the seepage abstraction by

considering different climate stages, climate scenarios, and introducing flow-focusing factors (BSC 2004 [DIRS 169131], Section 6.6.5). Seepage is calculated in the TSPA-LA using percolation flux distributions based on results from the UZ flow and transport model (BSC 2004 [DIRS 169131], Section 6.6.5.1), given in DTNs: LB0302PTNTSW9I.001 [DIRS 162277] and LB0305PTNTSW9I.001 [DIRS 163690]. These flux distributions include different climate stages and scenarios. The potential focusing of flow towards individual drift sections is accounted for by a distribution of flow-focusing factors, as discussed in *Abstraction of Drift Seepage* (BSC 2004 [DIRS 169131], Section 6.6.5.2). This distribution is given in DTN: LB0406U0075FCS.002 [DIRS 170712]. The local percolation flux distribution used for the seepage calculations in the TSPA-LA is derived by multiplying the percolation flux values from the site-scale model with the randomly sampled flow-focusing factors (BSC 2004 [DIRS 169131], Section 6.7.1).

The potential increase in the magnitude of percolation flux at the repository, as a result of climate changes, is accounted for in the THC seepage model by implicitly considering different climate stages, and climate scenarios when setting infiltration rates at the top model boundary (BSC 2004 [DIRS 172463], Sections 6.2.1.3 and 6.5.2). Also, flux increases caused by reflux of water upon boiling are explicitly accounted for by the modeling of coupled THC processes (BSC 2004 [DIRS 172463], Sections 6.2.1 and 6.5.5.2). Therefore, these effects are directly accounted for in results from the THC seepage model and their abstraction (BSC 2004 [DIRS 169858], Section 6.2). Summary tables of concentrations through time are presented in DTNs: LB0302DSCPTHCS.002 [DIRS 161976], LB0307DSTTHCR2.002 [DIRS 165541], and summary statistics through time are presented in LB0311ABSTHCR2.001 [DIRS 166714]. DTNs: LB0302DSCPTHCS.002 [DIRS 161976] and LB0311ABSTHCR2.001 [DIRS 166714] are used to feed and/or provide technical basis for *Engineered Barrier System: Physical and Chemical Environment Model* (BSC 2004 [DIRS 169860]), which generates lookup tables used in the TSPA-LA model. Note that seepage is calculated in the TSPA-LA using percolation flux distributions that are based on results from the UZ flow and transport model (BSC 2004 [DIRS 169131], Section 6.6.5.1), given in DTNs: LB0302PTNTSW9I.001 [DIRS 162277] and LB0305PTNTSW9I.001 [DIRS 163690]. These flux distributions include the same climate stages and scenarios as used in the THC seepage model.

Waste heat causes water to boil and move as vapor to a cooler region where it condenses. This condensation is then available to increase the percolation flux. The effect of this increased percolation flux at the repository as a result of this refluxing flow was examined in *Drift-Scale Coupled Processes (DST and TH Seepage) Models* (BSC 2004 [DIRS 170338], Section 6.2.2.2). Despite the refluxing of condensate, no seepage into intact drifts was found to occur as long as the temperature at the drift wall remains above 100°C. The thermal seepage abstraction for TSPA-LA consists of setting the thermal seepage for intact drifts equal to zero for the period of above-boiling temperatures at the drift wall. (For collapsed drifts and intact drifts with wall temperatures below 100°C, seepage is set equal to the estimated ambient seepage.)

Supporting Reports: *Simulation of Net Infiltration for Present-Day and Future Climates* (BSC 2004 [DIRS 170007]); *UZ Flow Models and Submodels* (BSC 2004 [DIRS 169861]); *Seepage Model for PA Including Drift Collapse* (BSC 2004 [DIRS 167652]); *Drift-Scale THC Seepage Model*, BSC 2004 [DIRS 172463]; *Abstraction of Drift Seepage*, BSC 2004 [DIRS 169131]; *Particle Tracking Model and Abstraction of Transport Process* (BSC 2004

[DIRS 170041]); *Drift-Scale Coupled Processes (DST and TH Seepage) Models*, (BSC 2004 [DIRS 170338]).

6.2.8 Enhanced Influx at the Repository (2.1.08.02.0A)

FEP Description: An opening in unsaturated rock may alter the hydraulic potential, affecting local saturation around the opening and redirecting flow. Some of the flow may be directed to the opening where it is available to seep into the opening.

Screening Decision: Included.

TSPA Disposition: The impact of an underground opening on the unsaturated flow field (including capillary barrier effect and flow diversion around the drifts) and its relevance for seepage is explicitly captured in the seepage process models used for the seepage abstraction *Seepage Model for PA Including Drift Collapse* (BSC 2004 [DIRS 167652], Section 6.3), *Abstraction of Drift Seepage* (BSC 2004 [DIRS 169131], Sections 6.4.1, 6.4.2, and 6.4.3); and *Drift-Scale Coupled Processes (DST and TH Seepage) Models* (BSC 2004 [DIRS 170338] Sections 6.1.1 and 6.2.1.4). Parameters used in the process models are developed from inverse modeling in *Seepage Calibration Model and Seepage Testing Data*, BSC 2004 [DIRS 171764], Sections 6.3, 6.6, and 6.8). From these model simulations, seepage predictions are available in the form of look-up tables in DTNs: LB0304SMDCREV2.002 [DIRS 163687] and LB0307SEEPDRCL.002 [DIRS 164337]. These will be used in the TSPA-LA to calculate ambient seepage, by sampling parameter cases of seepage-relevant parameters from the probability distributions that are defined in *Abstraction of Drift Seepage* (BSC 2004 [DIRS 169131], Section 6.7.1). These seepage-relevant parameters are the effective capillary-strength parameter, the permeability, and the local percolation flux. The percolation flux distributions include flow-focusing effects, as discussed in *Abstraction of Drift Seepage* (BSC 2004 [DIRS 169131], Section 6.6.5.2). During the thermal period, the ambient seepage rates will be adjusted based on the TH-modeling results from DTN: LB0301DSCPTHSM.002 [DIRS 163689], using the abstraction methodology developed in *Abstraction of Drift Seepage* (BSC 2004 [DIRS 169131], Sections 6.5.2 and 6.5.3).

Supporting Reports: *Seepage Model for PA Including Drift Collapse* (BSC 2004 [DIRS 167652]); *Seepage Calibration Model and Seepage Testing Data* (BSC 2004 [DIRS 171764]); *Abstraction of Drift Seepage* (BSC 2004 [DIRS 169131]); *Drift-Scale Coupled Processes (DST and TH Seepage) Models* (BSC 2004 [DIRS 170338]).

6.2.9 Mechanical Effects of Excavation and Construction in the Near-Field (2.2.01.01.0A)

FEP Description: Excavation will produce some disturbance of the rocks surrounding the drifts due to stress relief. Stresses associated directly with excavation (e.g., boring and blasting operations) may also cause some changes in rock properties. Properties that may be affected include rock strength, fracture spacing and block size, and hydrologic properties such as permeability.

associated with the grid used for the UZ flow model, the stratigraphy information is implicitly embedded in the TSPA-LA through the output flow fields. Aspects that affect hydrogeologic properties for flow are further discussed in *Development of Numerical Grids for UZ Flow and Transport Modeling* (BSC 2004 [DIRS 169855], Section 6) and *Calibrated Properties Model* (BSC 2004 [DIRS 169857], Section 6.1.4). See also FEP 2.2.03.02.0A.

This FEP is also implicitly included for radionuclide transport in the UZ through the use of pregenerated flow fields (DTN: LB0305TSPA18FF.001 [DIRS 165625]) as used by FEHM in TSPA-LA UZ multirealization runs as described in *Particle Tracking Model and Abstraction of Transport Processes* (BSC 2004 [DIRS 170041], Section 6.5.1). However, *Particle Tracking Model and Abstraction of Transport Processes* (BSC 2004 [DIRS 170041]) provides a model for use in TSPA-LA, but does not generate a direct data feed to TSPA-LA pertaining to this FEP.

Ambient seepage as a result of incomplete flow diversion around drifts is a local process simulated by drift-scale seepage process models (BSC 2004 [DIRS 169131], Section 6.4). In these models, the stratigraphy below and above the repository unit can be neglected. In contrast, the UZ flow and transport model (which provides the percolation flux distributions used for seepage calculations) explicitly accounts for the various geological units and major faults in the UZ (BSC 2004 [DIRS 169861], Sections 6.1.1 and 6.1.2). This is because the overall distribution of percolation flux at the repository horizon is influenced by stratigraphic layering and by major discontinuities. For example, the PTn unit overlying the Topopah Spring welded tuff units can divert a fraction of percolating water to intercepting faults and fault zones, thereby changing the spatial distribution of fluxes (BSC 2004 [DIRS 169861], Section 6.6.3), which could affect water-rock interaction and seepage water chemistry. The drift-scale process models addressing TH, THM, and THC processes (BSC 2004 [DIRS 169131], Sections 6.4.3.1, 6.4.4.1, and 6.4.4.2) also represent the stratigraphy in the UZ at Yucca Mountain in an explicit manner. This is needed because the thermal perturbation of the unsaturated rock extends far into the overlying and underlying geological units. Thus, the stratigraphy information is inherently embedded in the respective model results from the UZ flow and transport model and the TH, THM, and THC drift-scale models. Also, the mineralogy of stratigraphic intervals affects seepage water chemistry. For example, the presence of fluorite in the Tptpl hydrogeologic unit may affect fluoride concentrations in porewaters in this unit (BSC 2004 [DIRS 172463], Section 6.5.5.2). Finally, the thermal perturbation of the unsaturated rock extends far into the geologic units overlying and underlying the emplacement drifts. For these reasons, the THC seepage model includes explicitly the Yucca Mountain stratigraphy (BSC 2004 [DIRS 172463], Sections 4.1.2 and 6.5.1), using stratigraphic information from DTN: LB990501233129.004 [DIRS 111475] and mineralogical information from DTNs: LA9908JC831321.001 [DIRS 113495], LA9912SL831151.001 [DIRS 146447], LA9912SL831151.002 [DIRS 146449], and LA0009SL831151.001 [DIRS 153485]. Therefore, the results from the THC seepage model, and their abstraction in *Post-Processing Analysis for THC Seepage* (BSC 2004 [DIRS 169858], Section 6.2), explicitly account for the effect of stratigraphy on predicted water and gas chemistry. Summary tables of concentrations through time are presented in DTNs: LB0302DSCPTHCS.002 [DIRS 161976], LB0307DSTTHCR2.002 [DIRS 165541], and summary statistics through time are presented in LB0311ABSTHCR2.001 [DIRS 166714]. These data are used to feed and/or provide technical basis for *Engineered Barrier System: Physical and Chemical Environment Model* (BSC 2004 [DIRS 169860]), which generates look-up tables used in the TSPA-LA model.

The bases for the UZ and SZ stratigraphic models are different. The UZ uses the geologic framework model, GFM2000 (BSC 2004 [DIRS 170029]); DTN: MO0012MWDGFM02.002 [DIRS 153777]) and the SZ uses the hydrogeologic framework model, HFM (BSC 2004 [DIRS 170008]; DTN: GS000508312332.002 [DIRS 150136]). These different models for stratigraphy are used as a result of the different domains treated by the UZ and SZ models. The UZ model encompasses rock above the water table over a region around the repository that is roughly 5 km × 9 km (BSC 2004 [DIRS 169861], Figure 6.1-1). The SZ model encompasses rock below the water table over an area that is roughly 30 km × 45 km (BSC 2004 [DIRS 170037], Figure 6-1).

Stratigraphy is implicitly incorporated in the output from reports that develop different data sets for drifts in the Tptpl and Tptpmn. This includes *Drift-Scale Coupled Processes (DST and TH Seepage) Models* (BSC 2004 [DIRS 170338]) and *Seepage Model for PA Including Drift Collapse* (BSC 2004 [DIRS 167652], Sections 6.3.2 through 6.3.4). Stratigraphy is also explicitly incorporated in *Analysis of Hydrologic Properties Data* (BSC 2004 [DIRS 170038]). Stratigraphy is implicitly incorporated in *Simulation of Net Infiltration for Present-Day and Future Climates* (BSC 2004 [DIRS 170007], Section 6.6) because different strata form the bedrock at different locations.

Supporting Reports: *Development of Numerical Grids for UZ Flow and Transport Modeling* (BSC 2004 [DIRS 169855]); *Calibrated Properties Model* (BSC 2004 [DIRS 169857]); *UZ Flow Models and Submodels* (BSC 2004 [DIRS 169861]); *Seepage Model for PA Including Drift Collapse* (BSC 2004 [DIRS 167652]); *Analysis of Hydrologic Properties Data* (BSC 2004 [DIRS 170038]); *Drift-Scale THC Seepage Model* (BSC 2004 [DIRS 172463]); *Abstraction of Drift Seepage* (BSC 2004 [DIRS 169131]); *Drift-Scale Coupled Processes (DST and TH Seepage) Models* (BSC 2004 [DIRS 170338]); *Simulation of Net Infiltration for Present-Day and Potential Future Climate* (BSC 2004 [DIRS 170007]); *Particle Tracking Model and Abstraction of Transport Processes* (BSC 2004 [DIRS 170041]).

6.2.11 Rock Properties of Host Rock and Other Units (2.2.03.02.0A)

FEP Description: Physical properties such as porosity and permeability of the relevant rock units, soils, and alluvium are necessary for the performance assessment. Possible heterogeneities in these properties should be considered. Questions concerning events and processes that may cause these physical properties to change over time are considered in other FEPs.

Screening Decision: Included.

TSPA Disposition: This FEP is similar to FEP 2.2.03.01.0A, Stratigraphy (Section 6.2.10). Rock properties used are defined for each of the stratigraphic units/layers classified in the geological framework model (GFM2000; MO0012MWDGFM02.002 [DIRS 153777]), which is further developed into model grid in *Development of Numerical Grids for UZ Flow and Transport Modeling* (BSC 2004 [DIRS 169855]). However, rock properties are not developed in the grid development report. For the UZ flow model rock properties are modeled in terms of the sequence of hydrogeologic units and discrete faults (BSC 2004 [DIRS 169861], Section 6.1.5). Therefore, rock properties are implicitly embedded in the TSPA-LA through the output flow fields, with site-scale layering and faults explicitly taken into account. Rock properties used as

input for *UZ Flow Models and Submodels* (BSC 2004 [DIRS 169861]) are developed in *Calibrated Properties Model* (BSC 2004 [DIRS 169857], Section 6.3). On the drift scale, the effects of rock heterogeneity on seepage are discussed in *Abstraction of Drift Seepage* (BSC 2004 [DIRS 169131]). Percolation-flux distributions provided by *UZ Flow Models and Submodels* (BSC 2004 [DIRS 169861]) are used in *Abstraction of Drift Seepage* (BSC 2004 [DIRS 169131], Section 6.6.5.1), which accounts for rock properties and their variation on a larger scale (e.g., stemming from stratigraphy effects).

Rock properties of host rock and other units are included and used in the simulations of radionuclide transport through the UZ. *Particle Tracking Model and Abstraction of Transport Processes* (BSC 2004 [DIRS 170041], Sections 6.5.3 and 6.5.7) documents the matrix porosity, rock density, fracture porosity, fracture spacing, and aperture data (DTNs: LB0305TSPA18FF.001 [DIRS 165625], LB0210THRMLPRP.001 [DIRS 160799], LB0205REVUZPRP.001 [DIRS 159525], and LB0207REVUZPRP.001 [DIRS 159526]). The generated distributions of fracture porosity and fracture frequency are given in (DTN: LA0407BR831371.001 [DIRS 170806]) and will be used by TSPA-LA in multirealization runs as described in *Particle Tracking Model and Abstraction of Transport Processes* (BSC 2004 [DIRS 170041], Sections 6.5.3 and 6.5.7).

All the seepage process models that feed into seepage abstraction explicitly represent the physical properties of the unsaturated rock and their heterogeneity (BSC 2004 [DIRS 169131], Section 6.4). Small-scale heterogeneity is accounted for by a stochastic continuum representation of fracture permeability. Thus, heterogeneity on this scale is implicitly embedded in the model output from the seepage calibration model (BSC 2004 [DIRS 171764], Section 6.5.2), the seepage model for performance assessment (BSC 2004 [DIRS 167652], Sections 6.3.2 through 6.3.4), and the TH seepage model (BSC 2004 [DIRS 170338]) provided respectively in DTNs: LB0304SMDCREV2.002 [DIRS 163687]; LB0307SEEPDRCL.002 [DIRS 164337]; and LB0301DSCPTHSM.002 [DIRS 163689]. The intermediate-scale spatial variability and uncertainty of seepage-relevant rock properties are accounted for by appropriate probability distributions that were developed in *Abstraction of Drift Seepage* (BSC 2004 [DIRS 169131], Sections 6.6.1 and 6.6.2). Potential alterations of these properties, as a result of THM or THC processes, have been assessed using drift-scale process models (BSC 2004 [DIRS 169131], Sections 6.4.4.1 and 6.4.4.2). It was demonstrated that these potential alterations can be neglected in the TSPA-LA, because the expected changes would lead to less seepage (BSC 2004 [DIRS 169131], Section 6.5.1.4; see FEPs 2.1.09.12.0A and FEP 2.2.10.04.0A). The THC seepage model feeding into the drift-scale coupled process abstraction model explicitly represents the physical properties of the unsaturated rock (BSC 2004 [DIRS 172463], Section 6.4.7 and Table 6.4-1). Therefore, these effects are explicitly accounted for in the results from the THC seepage model, and their abstraction in *Post-Processing Analysis for THC Seepage* (BSC 2004 [DIRS 169858], Section 6.2). Summary tables of concentrations through time are presented in DTNs: LB0302DSCPTHCS.002 [DIRS 161976], LB0307DSTTHCR2.002 [DIRS 165541], and summary statistics through time are presented in LB0311ABSTHCR2.001 [DIRS 166714]. These data are used to feed and/or provide technical basis for *Engineered Barrier System: Physical and Chemical Environment Model* (BSC 2004 [DIRS 169860]), which generates lookup tables used in the TSPA-LA model. Small-scale fracture permeability heterogeneity was also investigated and determined not to significantly affect seepage water chemistry (BSC 2004 [DIRS 172463], Section 6.3). The THC seepage

model includes rock properties from DTNs: LB0205REVUZPRP.001 [DIRS 159525], LB0208UZDSCPMI.002 [DIRS 161243], LB0207REVUZPRP.002 [DIRS 159672] and LB0210THRMLPRP.001 [DIRS 160799]. Potential alterations of these properties as a result of THC processes are explicitly accounted for by the modeling of coupled THC processes, and result in reducing fracture permeability (BSC 2004 [DIRS 172463], Section 6.5.5.3). The effects of rock properties are also included in the treatment of infiltration uncertainty for TSPA-LA (BSC 2003 [DIRS 165991]). Infiltration uncertainty is represented through three discrete infiltration scenarios (lower, mean, and upper), which are sampled in TSPA-LA according to weighting factors (BSC 2003 [DIRS 165991], Section 7.1). Rock properties are included through the fracture parameters bedrock permeability (BRPERM) and bedrock porosity (BRPOROS). The uncertainties for these parameters are described in *Analysis of Infiltration Uncertainty* (BSC 2003 [DIRS 165991], Tables 6-2 and 6-3). These uncertainties are propagated through the infiltration numerical model and so are implicitly included in the output (weighting factors) that is passed to TSPA-LA (BSC 2003 [DIRS 165991]; DTN: SN0308T0503100.008 [DIRS 165640]). Heterogeneities in these properties are included in the input used in the analysis reported in *Simulation of Net Infiltration for Present-Day and Potential Future Climates* (BSC 2004 [DIRS 170007], Section 6.6.4 and Appendix B).

Rock properties are implicitly incorporated in the output from reports that develop different data sets for drifts in the Tptpl and Tptpmn. This includes *Drift-Scale Coupled Processes (DST and TH Seepage) Models* (BSC 2004 [DIRS 170338]) and *Seepage Model for PA Including Drift Collapse* (BSC 2004 [DIRS 167652], Sections 6.3.2 through 6.3.4). Rock properties are also explicitly incorporated in *Analysis of Hydrologic Properties Data* (BSC 2004 [DIRS 170038]). Rock properties are implicitly incorporated in *Simulation of Net Infiltration for Present-Day and Potential Future Climate* (BSC 2004 [DIRS 170007], Section 6.6.4 and Appendix B) and *Analysis of Infiltration Uncertainty* (BSC 2003 [DIRS 165991]) because different rocks form the bedrock at different locations.

Supporting Reports: *UZ Flow Models and Submodels* (BSC 2004 [DIRS 169861]); *Simulation of Net Infiltration for Present-Day and Potential Future Climates* (BSC 2004 [DIRS 170007]); *Calibrated Properties Model* (BSC 2004 [DIRS 169857]); *Abstraction of Drift Seepage* (BSC 2004 [DIRS 169131]); *Particle Tracking Model and Abstraction of Transport Processes* (BSC 2004 [DIRS 170041]); *Seepage Model for PA Including Drift Collapse* (BSC 2004 [DIRS 167652]); *Seepage Calibration Model and Seepage Testing Data* (BSC 2004 [DIRS 171764]); *Analysis of Hydrologic Properties Data* (BSC 2004 [DIRS 170038]); *Drift-Scale THC Seepage Model* (BSC 2004 [DIRS 172463]); *Drift-Scale Coupled Processes (DST and TH Seepage) Models* (BSC 2004 [DIRS 170338]); *Analysis of Infiltration Uncertainty* (BSC 2003 [DIRS 165991]).

6.2.12 Locally Saturated Flow at Bedrock/Alluvium Contact (2.2.07.01.0A)

FEP Description: In washes in arid areas, infiltration can descend to the alluvium/bedrock interface and then proceed down the wash at that interface as a saturated flow system distinct from the surface and distinct from the local water table.

Screening Decision: Included.

[DIRS 172463], Section 6.2.1). Therefore, the results from the THC seepage model, and their abstraction in *Post-Processing Analysis for THC Seepage* (BSC 2004 [DIRS 169858], Section 6.2), explicitly account for the effect of unsaturated groundwater flow on predicted water and gas chemistry. Summary tables of concentrations through time are presented in DTNs: LB0302DSCPTHCS.002 [DIRS 161976], LB0307DSTTHCR2.002 [DIRS 165541]), and summary statistics through time are presented in LB0311ABSTHCR2.001 [DIRS 166714]. These data are used to feed and/or provide technical basis for *Engineered Barrier System: Physical and Chemical Environment Model* (BSC 2004 [DIRS 169860]), which generates look-up tables used in the TSPA-LA model.

Supporting Reports: *In Situ Field Testing of Processes* (BSC 2004 [DIRS 170004]); *Simulation of Net Infiltration for Present-Day and Potential Future Climates* (BSC 2004 [DIRS 170007]); *UZ Flow Models and Submodels* (BSC 2004 [DIRS 169861]); *Conceptual Model and Numerical Approaches for UZ Flow and Transport* (BSC 2004 [DIRS 170035]); *Calibrated Properties Model* (BSC 2004 [DIRS 169857]); *Seepage Model for PA Including Drift Collapse* (BSC 2004 [DIRS 167652]); *Seepage Calibration Model and Seepage Testing Data* (BSC 2004 [DIRS 171764]); *Analysis of Hydrologic Properties Data* (BSC 2004 [DIRS 170038]); *Drift-Scale THC Seepage Model* (BSC 2004 [DIRS 172463]); *Abstraction of Drift Seepage* (BSC 2004 [DIRS 169131]); *Drift-Scale Coupled Processes (DST and TH Seepage) Models* (BSC 2004 [DIRS 170338]); *Particle Tracking Model and Abstraction of Transport Processes* (BSC 2004 [DIRS 170041]).

6.2.14 Capillary Rise in the UZ (2.2.07.03.0A)

FEP Description: Capillary rise involves the drawing up of water, above the water table or above locally saturated zones, in continuous pores of the unsaturated zone until the suction gradient is balanced by the gravitational pull downward.

Screening Decision: Included.

TSPA Disposition: Capillary forces are included in the UZ flow model. These forces affect the distribution of water in the UZ through capillary effects on water flow, also known as capillary wicking. Parameters used for capillarity modeling are incorporated within the matrix properties (DTN: LB02091DSSCP3I.002 [DIRS 161433]) and fracture properties (DTN: LB0205REVUZPRP.001 [DIRS 159525]) as described in *UZ Flow Models and Submodels* (BSC 2004 [DIRS 169861], Section 6.2.5). These parameters are used as direct input to the UZ flow model and are implicitly incorporated into the output flow fields used in the TSPA-LA (output flow fields are in DTN: LB0305TSPA18FF.001 [DIRS 165625]).

Supporting Reports: *UZ Flow Models and Submodels* (BSC 2004 [DIRS 169861]).

6.2.15 Focusing of Unsaturated Flow (Fingers, Weeps) (2.2.07.04.0A)

FEP Description: Unsaturated flow can differentiate into zones of greater and lower saturation (fingers) that may persist as preferential flow paths. Heterogeneities in rock properties, including fractures and faults, may contribute to focusing. Focused flow may become locally saturated.

Screening Decision: Included.

TSPA Disposition: The UZ flow fields represent the redistribution of infiltration through UZ layers, with faults explicitly taken into account (BSC 2004 [DIRS 169861], Sections 6.1.2, 6.6.3, and 6.7.3). The flux redistribution is based on tuff layer properties including fracture and matrix interaction. Faults are included in the UZ flow model as discrete features; therefore, flow in faults is also included in the UZ flow model (BSC 2004 [DIRS 169861]). Flow model results indicate that as flow moves downward through the UZ, the flow tends to focus into fault zones, with the fraction of flow in the faults increasing from about 30–40 percent at the repository to about 60 percent at the water table (BSC 2004 [DIRS 169861], Section 6.6.3).

For radionuclide transport, the effect of focusing unsaturated flow is implicitly included through the use of pregenerated flow fields contained in DTN: LB0305TSPA18FF.001 [DIRS 165625] for simulations (BSC 2004 [DIRS 170041], Sections 6.5.1, 6.6.2). In TSPA-LA runs, pregenerated flow fields are used directly by the transport model FEHM (LANL 2003 [DIRS 165741]). *Particle Tracking Model and Abstraction of Transport Processes* (BSC 2004 [DIRS 170041]) provides a model for use in TSPA-LA, but does not generate a direct data feed to TSPA-LA pertaining to this FEP.

Intermediate-scale focusing of flow from the site scale to the drift scale is accounted for in the seepage abstraction by using appropriate flow-focusing factors (BSC 2004 [DIRS 169131], Section 6.6.5.2). The distribution of flow-focusing factors used for seepage calculations is developed in *Seepage Calibration Model and Seepage Testing Data* (BSC 2004 [DIRS 171764], Sections 6.3 and 6.6), using property values calibrated in *Calibrated Properties Model* (BSC 2004 [DIRS 169857], Sections 6.1.4 and 6.3.2). Small-scale preferential flow is explicitly simulated in the seepage process model, developed in *Seepage Model for PA Including Drift Collapse* (BSC 2004 [DIRS 167652], Section 6.8) that feeds into the abstraction by use of heterogeneous fracture-permeability fields (BSC 2004 [DIRS 169131], Sections 6.4.1.1, 6.4.2.1, and 6.4.3.1). Thus, preferential flow is inherently embedded in the seepage look-up tables for ambient seepage given in DTNs: LB0304SMDCREV2.002 [DIRS 163687] and LB0307SEEPDRCL.002 [DIRS 164337], and in the thermal seepage results provided in DTN: LB0301DSCPTHSM.002 [DIRS 163689]. The abstraction methodology for both ambient and thermal seepage is described in *Abstraction of Drift Seepage* (BSC 2004 [DIRS 169131], Section 6.7.1). The possibility of episodic finger flow is accounted for with an alternative conceptual model analyzed in the thermal seepage model report (BSC 2004 [DIRS 170338], Section 6.3). Results from this alternative conceptual model are consistent with results from the TH seepage model used for this abstraction (BSC 2004 [DIRS 169131], Section 6.4.3.2).

Intermediate-scale focusing of flow from the site scale to the drift scale is implicitly accounted for in *Drift-Scale Coupled Processes (DST and TH Seepage) Models* (BSC 2004 [DIRS 170338]) by using appropriate flow-focusing factors (BSC 2004 [DIRS 169131], Section 6.6.5.2). However, flow focusing is not taken into account in the THC seepage model results or their abstraction (BSC 2004 [DIRS 169858], Section 6.2). This is because fracture permeability heterogeneity was determined to not significantly affect seepage water chemistry (BSC 2004 [DIRS 172463], Section 6.3). DTNs: LB0302DSCPTHCS.002 [DIRS 161976] and LB0311ABSTHCR2.001 [DIRS 166714] are used to feed and/or provide technical basis for *Engineered Barrier System: Physical and Chemical Environment Model* (BSC 2004

[DIRS 169860]), which generates look-up tables used in the TSPA-LA model. Another aspect of flow focusing is the channeling of fracture flow into a relatively few fractures. This is captured in the active fracture model described and validated in *Conceptual Model and Numerical Approaches for UZ Flow and Transport* (BSC 2004 [DIRS 170035], Sections 6.1.7 and 6.3.7, description; Section 7, validation). The active-fracture parameter values for different model layers are calibrated in the *Calibrated Properties Model* (BSC 2004 [DIRS 169857], Tables 6-8, 6-9, 6-10, and 6-14).

Supporting Reports: *Conceptual Model and Numerical Approaches for UZ Flow and Transport* (BSC 2004 [DIRS 170035]); *Calibrated Properties Model* (BSC 2004 [DIRS 169857]); *UZ Flow Models and Submodels* (BSC 2004 [DIRS 169861]); *Seepage Model for PA Including Drift Collapse* (BSC 2004 [DIRS 167652]); *Seepage Calibration Model and Seepage Testing Data* (BSC 2004 [DIRS 171764]); *Drift-Scale Coupled Processes (DST and TH Seepage) Models* (BSC 2004 [DIRS 170338]); and *Abstraction of Drift Seepage* (BSC 2004 [DIRS 169131]); *Particle Tracking Model and Abstraction of Transport Processes* (BSC 2004 [DIRS 170041]); *Drift-Scale THC Seepage Model* (BSC 2004 [DIRS 172463]).

6.2.16 Long-Term Release of Radionuclides from the Repository (2.2.07.06.0B)

FEP Description: The release of radionuclides from the repository may occur over a long period of time, as a result of the timing and magnitude of the waste packages and drip shield failures, waste form degradation, and radionuclide transport through the invert.

Screening Decision: Included.

TSPA Disposition: The effects of long-term waste package failures over a long period of time are included in the source term model for TSPA-LA (BSC 2003 [DIRS 166296], Section 5.1). This is done by modeling the environmental conditions of the waste packages in different parts of the repository and by modeling corrosion processes under these environmental conditions that lead to waste package failure. Releases from the waste package and engineered barrier system serve as a time-dependent boundary condition to the mountain-scale radionuclide transport model, which allows for a general time-dependent radionuclide source term that accounts for long-term releases (BSC 2004 [DIRS 170041], Section 6.4.7). For each GoldSim-FEHM run, GoldSim passes radionuclide mass releases to FEHM and FEHM simulates the transport process through the UZ. Long-term radionuclide release because of the failure of waste packages in the repository is implicitly included in *Particle Tracking Model and Abstraction of Transport Processes* (BSC 2004 [DIRS 170041], Sections 6.4.6 and 6.4.7). *Particle Tracking Model and Abstraction of Transport Processes* (BSC 2004 [DIRS 170041]) provides a model for use in TSPA-LA, but does not generate a direct data feed to TSPA-LA pertaining to this FEP.

Supporting Reports: *Particle Tracking Model and Abstraction of Transport Processes* (BSC 2004 [DIRS 170041]).

6.2.17 Perched Water Develops (2.2.07.07.0A)

FEP Description: Zones of perched water may develop above the water table. If these zones occur above the repository, they may affect UZ flow between the surface and the waste

Models and Submodels (BSC 2004 [DIRS 169861], Table 4.1-1). Permeabilities and other properties are calibrated as described in the *Analysis of Hydrologic Properties Data* (BSC 2004 [DIRS 170038]) and *Calibrated Properties Model* (BSC 2004 [DIRS 169857], Sections 6.1.4 and 6.3). The fracture-continuum properties are used as inputs to the UZ flow model, and their effects are incorporated into the output flow fields developed for use in TSPA-LA (output flow fields are in DTN: LB0305TSPA18FF.001 [DIRS 165625]). Output flow fields for the fracture continuum are presented in *UZ Flow Models and Submodels* (BSC 2004 [DIRS 169861], Section 6.6.3)

The top boundary condition for the UZ flow model is set by the infiltration maps output by *Simulation of Net Infiltration for Present-Day and Potential Future Climates* (BSC 2004 [DIRS 170007], Section 6.11). When the soil/bedrock contact reaches near-saturated conditions, fracture flow is initiated in the bedrock (BSC 2004 [DIRS 170007]) Sections 6.1.2 and 6.3.4). Channeling in the UZ fracture continuum is captured as discussed for FEP 2.2.07.04.0A, including the use of the active fracture model in *Conceptual Model and Numerical Approaches for UZ Flow and Transport* (BSC 2004 [DIRS 170035], Section 6.3); and the development of the distribution of flow-focusing factors in *Seepage Calibration Model and Seepage Testing Data* (BSC 2004 [DIRS 171764], Sections 6.3 and 6.6).

In the UZ, fracture flow plays an important role in the transport of radionuclides. In TSPA-LA runs, the effect of fracture flow on radionuclide transport (advection) is implicitly included through FEHM's use of pregenerated flow fields (DTN: LB0305TSPA18FF.001 [DIRS 165625]) in UZ transport simulations as described in *Particle Tracking Model and Abstraction of Transport Processes* (BSC 2004 [DIRS 170041], Section 6.5.1). *Particle Tracking Model and Abstraction of Transport Processes* (BSC 2004 [DIRS 170041]) provides a model for use in TSPA-LA, but does not generate a direct data feed to TSPA-LA pertaining to this FEP.

Flow processes in fractures or other channels are important for the seepage abstraction, because the amount of seepage is determined by the capacity of the fracture network to divert flow around the drifts as a result of capillary forces (*Abstraction of Drift Seepage*, BSC 2004 [DIRS 169131], Section 6.3.1). All the seepage process models that feed into seepage abstraction simulate flow processes in fractured rock (BSC 2004 [DIRS 169131], Section 6.4). Spatial variability in the fracture flow, potentially leading to water flow through only a portion of the fracture network, is accounted for by using a stochastic continuum representation. For ambient seepage, the fracture flow processes in the drift vicinity and the resulting seepage rates are predicted by model simulations from the seepage model for PA (BSC 2004 [DIRS 167652], Sections 6.3.2 and 6.3.3) and abstracted in *Abstraction of Drift Seepage* (BSC 2004 [DIRS 169131], Section 6.4.2). Results are available as look-up tables in DTNs: LB0304SMDCREV2.002 [DIRS 163687] and LB0307SEEPDRCL.002 [DIRS 164337]. These will be used in the TSPA-LA to calculate ambient seepage, by sampling parameter cases of seepage-relevant parameters from the probability distributions defined in Section 6.7.1 of *Abstraction of Drift Seepage* (BSC 2004 [DIRS 169131]). During the thermal period, the ambient seepage rates will be adjusted based on the TH-modeling results from *Drift-Scale Coupled Processes (DST and TH Seepage) Models* (BSC 2004 [DIRS 170338]), which explicitly simulates thermally perturbed fracture flow conditions. Results are given in

DTN: LB0301DSCPTHSM.002 [DIRS 163689]. The abstraction methodology for thermal seepage is developed in *Abstraction of Drift Seepage* (BSC 2004 [DIRS 169131]), Section 6.5.2). THM and THC effects on fracture flow processes are evaluated with process models that explicitly account for fracture flow affected by THM and THC parameter alterations (BSC 2004 [DIRS 169131], Section 6.4.4). It was demonstrated that these potential alterations can be neglected in the TSPA-LA, because the expected changes would lead to less seepage (BSC 2004 [DIRS 169131], Section 6.5.1.4; Sections 6.9.1 (FEP 2.1.09.12.0A) and 6.9.10 (FEP 2.2.10.04.0A). Percolation flux distributions are provided by the UZ flow model for use in the seepage abstraction model (BSC 2004 [DIRS 169131], Section 6.6.5.1), which accounts for fracture flow on a larger scale (influenced by climate changes), infiltration variability, and stratigraphy effects. Flow focusing effects (channeling) are included as discussed in *Abstraction of Drift Seepage* (BSC 2004 [DIRS 169131], Section 6.6.5.2).

Flow processes in fractures or other channels affect modeled THC coupled processes because of (1) their strong effect on TH behavior (BSC 2004 [DIRS 169131], Section 6.4.4) and (2) their strong effect on water and gas chemistry (BSC 2004 [DIRS 172463], Section 6.2.1). The latter is primarily due to volatilization of steam and CO₂ from the rock matrix-water and subsequent transport and condensation in fractures. The amount of mobilized CO₂ with steam directly affects the pH of the condensate, which in turn affects the degree of water-rock interaction and water chemistry. These THC processes are influenced by the fracture characteristics, such as orientation, aperture, asperity, length, connectivity, and fillings. The THC seepage model that feeds into the drift scale coupled processes abstraction model explicitly simulate the flow processes in fractures using appropriate continuum properties that represent these characteristics as shown in *Drift-Scale THC Seepage Model* (BSC 2004 [DIRS 172463], Sections 6.4.3, 6.4.4, and 6.4.7). Thus, the results from the THC seepage model and their abstraction (BSC 2004 [DIRS 169858], Section 6.2), and tables of concentrations and summary statistics through time, implicitly account for the effect of climate change on THC processes. Summary tables of concentrations through time are presented in DTNs: LB0302DSCPTHCS.002 [DIRS 161976], LB0307DSTTHCR2.002 [DIRS 165541], and summary statistics through time are presented in LB0311ABSTHCR2.001 [DIRS 166714]. These data are used to feed and/or provide technical basis for *Engineered Barrier System: Physical and Chemical Environment Model* (BSC 2004 [DIRS 169860]) that generates lookup tables used in the TSPA-LA model. The effects of fracture flow are also included in the treatment of infiltration uncertainty for TSPA-LA (BSC 2003 [DIRS 165991]). Infiltration uncertainty is represented through three discrete infiltration scenarios (lower, mean, and upper), which are sampled in TSPA-LA according to weighting factors (BSC (2003 [DIRS 165991], Section 7.1). This FEP is implicitly included in the determination of the weighing factors fed to TSPA-LA (BSC 2003 [DIRS 165991]; DTN: SN0308T0503100.008 [DIRS 165640]). This FEP is incorporated in the uncertain parameters describing the bedrock permeability multiplier (BRPERM) and bedrock porosity (BRPOROS).

Supporting Reports: *In Situ Field Testing of Processes* (BSC 2004 [DIRS 170004]); *Simulation of Net Infiltration for Present-Day and Potential Future Climates* (BSC 2004 [DIRS 170007]); *Conceptual Model and Numerical Approaches for UZ Flow and Transport* (BSC 2004 [DIRS 170035]); *Analysis of Hydrologic Properties Data* (BSC 2004 [DIRS 170038]); *Calibrated Properties Model* (BSC 2004 [DIRS 169857]); *UZ Flow Models and Submodels* (BSC 2004 [DIRS 169861]); *Seepage Model for PA Including Drift Collapse*

(BSC 2004 [DIRS 167652]); *Seepage Calibration Model and Seepage Testing Data* (BSC 2004 [DIRS 171764]); *Drift-Scale THC Seepage Model* (BSC 2004 [DIRS 172463]); *Abstraction of Drift Seepage* (BSC 2004 [DIRS 169131]); *Drift-Scale Coupled Processes (DST and TH Seepage) Models* (BSC 2004 [DIRS 170338]); *Analysis of Infiltration Uncertainty* (BSC 2003 [DIRS 165991]); *Particle Tracking Model and Abstraction of Transport Processes* (BSC 2004 [DIRS 170041]).

6.2.19 Matrix Imbibition in the UZ (2.2.07.09.0A)

FEP Description: Water flowing in fractures or other channels in the unsaturated zone may be imbibed into the surrounding rock matrix. This may occur during steady flow, episodic flow, or into matrix pores that have been dried out during the thermal period.

Screening Decision: Included.

TSPA Disposition: Matrix imbibition is included in the process model for UZ flow at the mountain scale (BSC 2004 [DIRS 169861], Section 6.1.2). Matrix imbibition refers to the movement of water into the matrix as a result of capillary forces. This process affects the distribution of flow between fractures and matrix in a dual-permeability flow model for fractured rock. The flow simulations in *UZ Flow Models and Submodels* (BSC 2004 [DIRS 169861], Section 6.6) are for steady-state flow. Imbibition is captured in the UZ flow model through capillarity modeling, which uses matrix and fracture properties as model input. Therefore, the effect of imbibition is implicitly incorporated in the output flow fields (DTN: LB0305TSPA18FF.001 [DIRS 165625]) used in the TSPA-LA. Matrix imbibition is implicit in the increase in matrix saturation that is simulated when changing to a wetter climate state. Matrix imbibition is also important in damping the effect of episodic infiltration, as discussed in Appendix G of *UZ Flow Models and Submodel* (BSC 2004 [DIRS 169861]). Also see FEP 2.2.07.05.0A, Flow in the UZ from episodic infiltration.

For TSPA-LA runs, the pregenerated flow fields (DTN: LB0305TSPA18FF.001 [DIRS 165625]) are used by FEHM in UZ transport simulations as described in *Particle Tracking Model and Abstraction of Transport Processes* (BSC 2004 [DIRS 170041], Section 6.5.1). Therefore, the effects of matrix imbibition are implicitly included in the treatment of UZ radionuclide transport. However, *Particle Tracking Model and Abstraction of Transport Processes* provides a model for use in TSPA-LA, but does not generate a direct data feed to TSPA-LA.

The THC seepage model similarly explicitly accounts for matrix imbibition using appropriate dual-permeability modeling concepts as reported in *Drift-Scale THC Seepage Model* (BSC 2004 [DIRS 172463], Section 6.2.1). This is needed because heating and dryout of the unsaturated rock transfers liquid and gas from the matrix into the fractures; upon rewetting water and solutes are imbibed from fracture to matrix (see, for example, BSC 2004 [DIRS 172463], Figure 6.2-3). Therefore, these effects are directly accounted for in the results from the THC seepage model, and in their abstraction in *Post-Processing Analysis for THC Seepage* (BSC 2004 [DIRS 169858], Section 6.2). Summary tables of concentrations through time are presented in DTNs: LB0302DSCPTHCS.002 [DIRS 161976], LB0307DSTTHCR2.002 [DIRS 165541], and summary statistics through time are presented in LB0311ABSTHCR2.001 [DIRS 166714].

These data are used to feed and/or provide technical basis for *Engineered Barrier System: Physical and Chemical Environment Model* (BSC 2004 [DIRS 169860]), which generates look-up tables used in the TSPA-LA model.

Ambient seepage is mainly governed by flow in the fractures, as discussed in *Abstraction of Drift Seepage* (BSC 2004 [DIRS 169131], Section 6.4). Thus, in the predictive model for ambient seepage, that is, the seepage calibration model (BSC 2004 [DIRS 171764], Section 6.3.3.2) and the seepage model for PA (BSC 2004 [DIRS 167652], Section 6.3), matrix imbibition is neglected. In contrast, the drift-scale process models addressing TH, THM, and THC processes, including *Drift-Scale Coupled Processes (DST and TH Seepage) Models* (BSC 2004 [DIRS 170338]), *Drift-Scale THC Seepage Model* (BSC 2004 [DIRS 172463]), and *Abstraction of Drift Seepage* (BSC 2004 [DIRS 169131], Sections 6.4.3.1, 6.4.4.1, and 6.4.4.2), explicitly account for matrix imbibition using appropriate dual-permeability modeling concepts. This is needed because the thermal perturbation of the unsaturated rock results in significant transfer of liquid and gas from the matrix into the fractures and vice versa. The UZ flow model (which provides the percolation flux distributions used for seepage calculations) also accounts for the impact of matrix imbibition in an explicit manner (BSC 2004 [DIRS 169131], Section 6.6.5.1). Thus, matrix imbibition effects are inherently embedded in the respective model results used for this abstraction.

Matrix imbibition tests are reported in *In Situ Field Testing of Processes* (BSC 2004 [DIRS 170004], Section 6.4). The matrix properties used to simulate matrix imbibition are developed in *Calibrated Properties Model* (BSC 2004 [DIRS 169857], Section 6.1.5).

Supporting Reports: *In Situ Field Testing of Processes* (BSC 2004 [DIRS 170004]); *Calibrated Properties Model* (BSC 2004 [DIRS 169857]); *UZ Flow Models and Submodels* (BSC 2004 [DIRS 169861]); *Seepage Model for PA Including Drift Collapse* (BSC 2004 [DIRS 167652]); *Seepage Calibration Model and Seepage Testing Data* (BSC 2004 [DIRS 171764]); *Drift-Scale THC Seepage Model* (BSC 2004 [DIRS 172463]); *Abstraction of Drift Seepage* (BSC 2004 [DIRS 169131]); *Drift-Scale Coupled Processes (DST and TH Seepage) Models* (BSC 2004 [DIRS 170338]); *Particle Tracking Model and Abstraction of Transport Processes* (BSC 2004 [DIRS 170041]).

6.2.20 Condensation Zone Forms around Drifts (2.2.07.10.0A)

FEP Description: Condensation of the two-phase flow generated by repository heat may form in the rock where the temperature drops below the local vaporization temperature. Waste package emplacement geometry and thermal loading may affect the scale at which condensation caps form (over waste packages, over panels, or over the entire repository), and the extent to which “shedding” will occur as water flows from the region above one drift to the region above another drift or into the rock between drifts.

Screening Decision: Included.

TSPA Disposition: The coupled processes of vapor condensation forming a condensation zone (or “condensation cap”) in the fractured rock above the drifts are explicitly simulated with the TH seepage model (BSC 2004 [DIRS 170338], Sections 6.2 and 7.4) that feeds into the seepage

abstraction. Using this model, the impact of condensation and shedding on seepage is assessed for various simulation cases (BSC 2004 [DIRS 169131], Section 6.4.3.3). Thus, the TH-modeling results from DTN: LB0301DSCPTHSM.002 [DIRS 163689] inherently include these effects. As discussed in *Abstraction of Drift Seepage* (BSC 2004 [DIRS 169131], Section 6.5.2), the abstraction of thermal seepage uses these modeling results to develop an appropriate thermal-seepage abstraction methodology.

The coupled processes of vapor condensation forming a condensation cap above the drifts and occurrence of “shedding” between drifts (that is, diversion of vapor to cooler regions and drainage of condensation through the cooler region between drifts) are explicitly simulated with the THC seepage model (BSC 2004 [DIRS 172463], Sections 6.2.1, 6.5.5.1, 6.5.5.3, and 6.5.5.2.2). Using this model, the impact of condensation and drainage on seepage water chemistry is assessed for various simulation cases (BSC 2004 [DIRS 172463], Sections 6.2, 6.5, and 6.6). Therefore, the results from the THC seepage model, and their abstraction in *Post-Processing Analysis for THC Seepage* (BSC 2004 [DIRS 169858], Section 6.2), explicitly include these effects. Summary tables of concentrations through time are presented in DTNs: LB0302DSCPTHCS.002 [DIRS 161976], LB0307DSTTHCR2.002 [DIRS 165541], and summary statistics through time are presented in LB0311ABSTHCR2.001 [DIRS 166714]. These data are used to feed and/or provide technical basis for *Engineered Barrier System: Physical and Chemical Environment Model* (BSC 2004 [DIRS 169860]), which generates look-up tables used in the TSPA-LA model.

Supporting Reports: *Drift-Scale THC Seepage Model* (BSC 2004 [DIRS 172463]); *Abstraction of Drift Seepage*; (BSC 2004 [DIRS 169131]); *Post-Processing Analysis for THC Seepage* (BSC 2004 [DIRS 169858]); *Drift-Scale Coupled Processes (DST and TH Seepage) Models*; (BSC 2004 [DIRS 170338]).

6.2.21 Resaturation of Geosphere Dry-Out Zone (2.2.07.11.0A)

FEP Description: Following the peak thermal period, water in the condensation cap may flow downward into the drifts. Influx of cooler water from above, such as might occur from episodic flow, may accelerate return flow from the condensation cap by lowering temperatures below the condensation point. Percolating groundwater will also contribute to resaturation of the dry-out zone. Vapor flow, as distinct from liquid flow by capillary processes, may also contribute.

Screening Decision: Included.

TSPA Disposition: Resaturation of the dryout zone around drifts, and the potential of return flow from the condensation zone back to the drifts, are explicitly simulated with the TH seepage model (BSC 2004 [DIRS 170338], Section 6.2), which feeds into seepage abstraction. Using this model, the impact of resaturation and reflux (on) seepage is assessed for various simulation cases (BSC 2004 [DIRS 169131], Section 6.4.3.3). Thus, the TH-modeling results from DTN: LB0301DSCPTHSM.002 [DIRS 163689] inherently include these effects. As discussed in *Abstraction of Drift Seepage* (BSC (2004 [DIRS 169131], Section 6.5.2), the abstraction of thermal seepage utilizes these modeling results to develop an appropriate thermal-seepage abstraction methodology. The impact of potential episodic flow was addressed with an alternative conceptual model for thermal seepage, as discussed in *Abstraction of Drift Seepage*

(BSC 2004 [DIRS 169131], Section 6.4.3). It was shown that results from this alternative conceptual model are consistent with the process model results from the TH seepage model used for this abstraction.

Resaturation of the dryout zone around drifts, and the potential of return flow from the condensation zone back to the drifts, are explicitly simulated with the THC seepage model (BSC 2004 [DIRS 172463], Sections 6.2.1 and 6.5.5). Using this model, the impact of resaturation on reflux chemistry is assessed as part of the abstraction methodology (that is, the compositions of abstracted “FRONT” waters reflect concentration increases because of the dissolution of salts precipitated during dryout; see *Post-Processing Analysis for THC Seepage* (BSC 2004 [DIRS 169858], Section 6.2.3.1). Therefore, the results from the THC seepage model, and their abstraction in *Post-Processing Analysis for THC Seepage* (BSC 2004 [DIRS 169858], Section 6.2), explicitly include these effects. Summary tables of concentrations through time are presented in DTNs: LB0302DSCPTHCS.002 [DIRS 161976], LB0307DSTTHCR2.002 [DIRS 165541], and summary statistics through time are presented in LB0311ABSTHCR2.001 [DIRS 166714]. These data are used to feed and/or provide technical basis for *Engineered Barrier System: Physical and Chemical Environment Model* (BSC 2004 [DIRS 169860]), which generates look-up tables used in the TSPA-LA model.

Supporting Reports: *Drift-Scale THC Seepage Model* (BSC 2004 [DIRS 172463]); *Abstraction of Drift Seepage* (BSC 2004 [DIRS 169131]); *Post-Processing Analysis for THC Seepage* (BSC 2004 [DIRS 169858]); *Drift-Scale Coupled Processes (DST and TH Seepage) Models* (BSC 2004 [DIRS 170338]).

6.2.22 Advection and Dispersion in the UZ (2.2.07.15.0B)

FEP Description: Advection and dispersion processes may affect radionuclide transport in the UZ.

Screening Decision: Included.

TSPA Disposition: Radionuclide transport through the UZ by advection is simulated using the RTTF (Residence Time Transfer Function) method documented in *Particle Tracking Model and Abstraction of Transport Processes* (BSC 2004 [DIRS 170041], Section 6.4.1). Dispersion is incorporated into the RTTF algorithm through the use of a transfer function based on an analytical solution to the advection–dispersion equation (BSC 2004 [DIRS 170041], Section 6.4.2). In TSPA–LA runs, advection and dispersion are implicitly included through the use of FEHM RTTF model and the pregenerated flow fields as described in *Particle Tracking Model and Abstraction of Transport Processes* (BSC 2004 [DIRS 170041], Sections 6.4 and 6.5.1). *Particle Tracking Model and Abstraction of Transport Processes* (BSC 2004 [DIRS 170041]) provides a model for use in TSPA-LA, but does not generate a direct data feed to TSPA-LA pertaining to this FEP.

Supporting Reports: *Particle Tracking Model and Abstraction of Transport Processes* (BSC 2004 [DIRS 170041]).

drifts if the flux is sufficient to overcome the capillary barrier represented in the drift seepage model (BSC 2004 [DIRS 169131]); however, this FEP is not explicitly represented in that report. The lateral flow effect is implicitly incorporated in the output flow fields developed in *UZ Flow Models and Submodels* (BSC 2004 [DIRS 169861], Section 6.6.3) and submitted to the TDMS (DTN: LB0305TSPA18FF.001 [DIRS 165625]) for use in TSPA-LA. Other aspects of flow focusing in faults (preferential flow in faults) are discussed in FEP 2.2.07.04.0A. Perched water is discussed in FEP 2.2.07.07.0A.

Supporting Reports: *UZ Flow Models and Submodels* (BSC 2004 [DIRS 169861]).

6.2.25 Flow Diversion around Repository Drifts (2.2.07.20.0A)

FEP Description: Flow in unsaturated rock tends to be diverted by openings such as waste emplacement drifts due to the effects of capillary forces. The resulting diversion of flow could have an effect on seepage into the repository. Flow diversion around the drift openings could also lead to the development of a zone of lower flow rates and low saturation beneath the drift, known as the drift shadow.

Screening Decision: Included.

TSPA Disposition: The impact of flow diversion around the drifts and its relevance for seepage is explicitly captured in the data acquired in *In Situ Field Testing of Processes* (BSC 2004 [DIRS 170004], Section 6.2) and in the seepage process models (BSC 2004 [DIRS 171764], Sections 6.3, 6.6, and 6.8; BSC 2004 [DIRS 167652], Sections 6.2.1, 6.3.2, and 6.7; BSC 2004 [DIRS 170338]; BSC 2004 [DIRS 172463]) and the seepage abstractions (BSC 2004 [DIRS 169131], Sections 6.4.1, 6.4.2, and 6.4.3). From these model simulations, seepage predictions are available in the form of look-up tables in DTNs: LB0304SMDCREV2.002 [DIRS 163687] and LB0307SEEPDRCL.002 [DIRS 164337]. These will be used in the TSPA-LA to calculate ambient seepage, by sampling parameter cases of seepage-relevant parameters from the probability distributions defined in *Abstraction of Drift Seepage* (BSC 2004 [DIRS 169131], Section 6.7.1). These seepage-relevant parameters are the effective capillary-strength parameter permeability and local percolation flux. During the thermal period, the ambient rates will be adjusted based on the TH-modeling results from DTN: LB0301DSCPTHSM.002 [DIRS 163689], using the abstraction methodology developed in *Abstraction of Drift Seepage* (BSC 2004 [DIRS 169131], Section 6.5.2.1). The drift seepage model also captures the effects of drift collapse (BSC 2004 [DIRS 169131], Sections 6.4.2.4 and 6.7.1.2) in terms of the larger drift profile that results.

Supporting Reports: *In Situ Field Testing of Processes* (BSC 2004 [DIRS 170004]); *Seepage Model for PA Including Drift Collapse* (BSC 2004 [DIRS 167652]); *Seepage Calibration Model and Seepage Testing Data* (BSC 2004 [DIRS 171764]); *Drift-Scale THC Seepage Model* (BSC 2004 [DIRS 172463]); *Abstraction of Drift Seepage* (BSC 2004 [DIRS 169131]); *Drift-Scale Coupled Processes (DST and TH Seepage) Models* (BSC 2004 [DIRS 170338]).

6.2.26 Chemical Characteristics of Groundwater in the UZ (2.2.08.01.0B)

FEP Description: Chemistry and other characteristics of groundwater in the unsaturated zone may affect groundwater flow and radionuclide transport of dissolved and colloidal species.

Groundwater chemistry and other characteristics, including temperature, pH, Eh, ionic strength, and major ionic concentrations, may vary spatially throughout the system as a result of different rock mineralogy.

Screening Decision: Included.

TSPA Disposition: THC seepage model simulations feeding the drift scale coupled processes abstraction were run explicitly using five different input water compositions representing the range of compositions at Yucca Mountain (BSC 2004 [DIRS 172463], Table 6.2-1, Sections 6.2.2 and 6.5.5). This variability of porewater compositions in repository host units implicitly reflects spatial variations in rock mineralogy and infiltration rates. Therefore, the results from the THC seepage model, and their abstraction in *Post-Processing Analysis for THC Seepage* (BSC 2004 [DIRS 169858], Section 6.2), explicitly reflect the natural variability of porewater compositions and implicitly reflect the natural variability of rock mineralogy. Summary tables of concentrations through time are presented in DTNs: LB0302DSCPTHCS.002 [DIRS 161976], LB0307DSTTHCR2.002 [DIRS 165541], and summary statistics through time are presented in LB0311ABSTHCR2.001 [DIRS 166714]. These data are used to feed and/or provide technical basis for *Engineered Barrier System: Physical and Chemical Environment Model* (BSC 2004 [DIRS 169860]), which generates look-up tables used in the TSPA-LA model.

The effects of groundwater chemical characteristics are included in the radionuclide sorption coefficients under ambient conditions. The sorption coefficient data on which the distributions are based are obtained in laboratory experiments in which crushed rock samples from the Yucca Mountain site are contacted with groundwaters (or simulated groundwaters) representative of the site, spiked with one or more of the elements of interest (BSC 2004 [DIRS 164500], Sections A4 and A5). The chemistry of porewaters and perched waters in the UZ along potential flowpaths to the accessible environment is discussed in *Yucca Mountain Site Description* (BSC 2004 [DIRS 169734]). In the UZ, two distinct water types exist in the ambient system. One is perched water and the other is porewater. Perched water is generally more dilute than porewater. The J-13 and UE p#1 waters were used in sorption experiments as end-member compositions intended to bracket the impact of water composition on sorption coefficients (BSC 2004 [DIRS 164500], Section A4). Some spatial trends in water composition through the TSw and CHn geologic units have been noted (BSC 2003 [DIRS 169734], Section 5.2.2.4.2). However, the uncertainty in these spatial variations (BSC 2004 [DIRS 172463], Section 6.2.2.1) and the uncertainty with respect to the effects of the bounding water compositions on sorption (BSC 2004 [DIRS 164500], Sections A8.3, A8.4, and A8.9) have led to the treatment of natural variability in water composition as uncertainty. Sorption experiments have been carried out as a function of time, element concentration, atmospheric composition, particle size, and temperature. In some cases, the solids remaining from sorption experiments were contacted with unspiked groundwater in desorption experiments. The experimental data used to determine the sorption K_{ds} are provided in the following DTNs: LA0305AM831341.001 [DIRS 163789], LA0407AM831341.001 [DIRS 170623], LA0407AM831341.002 [DIRS 170621], LA0407AM831341.004 [DIRS 170622], LA0407AM831341.005 [DIRS 170625], LA0407AM831341.003 [DIRS 170626], LA0407AM831341.006 [DIRS 170628], and LA0310AM831341.001 [DIRS 165865]. The sorption and desorption experiments together provide information on the equilibration rates of the forward and backward sorption reactions.

For elements that sorb primarily through surface complexation reactions, the experimental data are augmented with the results of modeling calculations using PHREEQC (V2.3, STN: 10068-2.3-00) (BSC 2001 [DIRS 155323]). The inputs for the modeling calculations include groundwater compositions, surface areas, binding constants for the elements of interest, and thermodynamic data for solution species. These modeling calculations provide a basis for interpolation and extrapolation of the experimentally derived sorption coefficient dataset. The effects of nonlinear sorption are approximated by capturing the effective K_d range (BSC 2004 [DIRS 164500], Section A8).

The effects of groundwater composition with respect to sorption coefficients are provided in terms of probability distributions for the sorption coefficient of each element of interest among the three major rock types (devitrified, zeolitic, and vitric) found in the UZ. The influence of expected variations in water chemistry, radionuclide concentrations, and variations in rock surface properties within one of the major rock types are incorporated into these probability distributions. These distributions are specified for each radionuclide–rock type combination (BSC 2004 [DIRS 164500], Section I8) and are sampled in the TSPA-LA to account for the effects of natural variations in porewater chemistry and mineral surfaces on sorption. Correlations for sampling sorption coefficient probability distributions have been derived for the elements investigated (BSC 2004 [DIRS 164500], Appendix B). To derive the correlations, a rating system was first developed to rate the impact of six different variables on the sorption coefficient for a given element in each of the three major rock types. The six variables are pH, Eh, water chemistry, rock composition, rock surface area, and radionuclide concentration. Water chemistry refers to the major ion concentrations and silica. Rock composition refers to both the mineralogical composition of the rocks and the chemical composition of the minerals (for example, zeolite compositions). The output DTNs for the sorption K_d s and correlations are LA0408AM831341.001 [DIRS 171584] and LA0311AM831341.001 [DIRS 167015]. These K_d s, which include the effects of the chemical characteristics of groundwater, are used in the simulation of radionuclide transport for TSPA-LA, as described in *Particle Tracking Model and Abstraction of Transport Processes* (BSC 2004 [DIRS 170041], Section 6.5.4).

Supporting Reports: *Radionuclide Transport Models Under Ambient Conditions* (BSC 2004 [DIRS 164500]); *Particle Tracking Model and Abstraction of Transport Processes* (BSC 2004 [DIRS 170041]); *Drift-Scale THC Seepage Model* (BSC 2004 [DIRS 172463]).

6.2.27 Re-dissolution of Precipitates Directs More Corrosive Fluids to Waste Packages (2.2.08.04.0A)

FEP Description: Re-dissolution of precipitates that have plugged pores as a result of evaporation of groundwater in the dry-out zone, may produce a pulse of fluid reaching the waste packages when gravity-driven flow resumes, which is more corrosive than the original fluid in the rock.

Screening Decision: Included.

TSPA Disposition: The THC seepage model simulations feeding *Post-Processing Analysis for THC Seepage* (BSC 2004 [DIRS 169858]) explicitly consider the formation of salt precipitates upon dryout (BSC 2004 [DIRS 172463], Sections 6.4.5 and 6.5.5.2) and their dissolution during

rewetting around drifts (BSC 2004 [DIRS 172463], Section 6.5.5.2) and the resulting effect on percolation water chemistry (BSC 2004 [DIRS 169858], Section 6.2.3; BSC 2004 [DIRS 172463], Section 6.4.4). Therefore, the results from the THC seepage model, and their abstraction in *Post-Processing Analysis for THC Seepage* (BSC 2004 [DIRS 169858], Section 6.2), explicitly reflect the effect of salt redissolution upon rewetting. The effect results in an increase in both salinity and variability (BSC 2004 [DIRS 169858], Section 6.2.3). Summary tables of concentrations through time are presented in DTNs: LB0302DSCPTHCS.002 [DIRS 161976], LB0307DSTTHCR2.002 [DIRS 165541], and summary statistics through time are presented in LB0311ABSTHCR2.001 [DIRS 166714]. These data are used to feed and/or provide technical basis for *Engineered Barrier System: Physical and Chemical Environment Model* (BSC 2004 [DIRS 169860]), which generates look-up tables used in the TSPA-LA model.

Supporting Reports: *Drift-Scale THC Seepage Model* (BSC 2004 [DIRS 172463]); *Post-Processing Analysis for THC Seepage* (BSC 2004 [DIRS 169858]).

6.2.28 Complexation in the UZ (2.2.08.06.0B)

FEP Description: Complexing agents such as humic and fulvic acids present in natural groundwaters could affect radionuclide transport in the UZ.

Screening Decision: Included.

TSPA Disposition: Complexation on mobile complexing agents such as humic and fulvic acids is treated as part of colloid transport in *Radionuclide Transport Models Under Ambient Conditions* (BSC 2004 [DIRS 164500], Sections 6.1.3 and 6.18). Complexation on mineral surfaces is treated as part of sorption in *Radionuclide Transport Models Under Ambient Conditions* (BSC 2004 [DIRS 164500], Section A7). Therefore, the effects of complexation are implicitly included in the radionuclide sorption coefficients under ambient conditions. For TSPA-LA, radionuclide transport is simulated by a particle-tracking model that includes the effects of complexation, as described in *Particle Tracking Model and Abstraction of Transport Processes* (BSC 2004 [DIRS 170041], Section 6.5.4).

The sorption coefficient data on which the distributions are based are obtained in laboratory experiments in which crushed rock samples from the Yucca Mountain site are contacted with groundwaters (or simulated groundwaters) representative of the site (BSC 2004 [DIRS 164500], Section A4), spiked with one or more of the elements of interest (BSC 2004 [DIRS 164500], Section A5). As such, the sorption experiments contain representative ligands responsible for complex formation, such as carbonates (Triay et al. 1997 [DIRS 100422], p. 85, 133). Sorption experiments have been carried out as a function of time, element concentration, atmospheric composition, particle size, and temperature. In some cases, the solids remaining from sorption experiments were contacted with unspiked groundwater in desorption experiments. The experimental data used to determine the sorption K_d s are provided in the following DTNs: LA0305AM831341.001 [DIRS 163789], LA0407AM831341.001 [DIRS 170623], LA0407AM831341.002 [DIRS 170621], LA0407AM831341.004 [DIRS 170622], LA0407AM831341.005 [DIRS 170625], LA0407AM831341.003 [DIRS 170626], LA0407AM831341.006 [DIRS 170628], and LA0310AM831341.001 [DIRS 165865]. The

size (DTN: LL000122051021.116 [DIRS 142973]), colloid concentration (DTN: SN0306T0504103.005 [DIRS 164132]), radionuclide sorption coefficient onto colloid (DTN: SN0306T0504103.006 [DIRS 164131]), and colloid retardation factors (DTN: LA0303HV831352.002 [DIRS 163558]). The colloid concentration data and sorption-onto-colloid data are documented in *Waste Form and In-Drift Colloids-Associated Radionuclide Concentrations: Abstraction and Summary* (BSC 2004 [DIRS 170025], Section 6.3). Colloid retardation factors are documented in *Saturated Zone Colloid Transport* (BSC 2004 [DIRS 170006], Section 6.4.3). These data are used in *Particle Tracking Model and Abstraction of Transport Processes* (BSC 2004 [DIRS 170041], Sections 6.5.9 through 6.5.13). Colloid transport processes include advection and dispersion. In addition, colloids that undergo reversible filtration in fractures (BSC 2004 [DIRS 170041], Sections 6.4.5 and 6.5.9) are simulated through the use of the colloid retardation factor, R_c , which is evaluated based on field experiments in the C-Wells complex using microspheres as analogues. Field experiments have also shown that a small percentage of colloidal particles are transported through the groundwater system essentially unretarded (BSC 2004 [DIRS 170006], Section 6.6). The fractions of unretarded colloids have been developed based on field data (BSC 2004 [DIRS 170006]). Sorption of colloids is addressed in FEP 2.2.08.09.0B. Colloid matrix diffusion was assumed not to occur because its effect would be small and would only retard transport (BSC 2004 [DIRS 170041], Section 6.5.5). Therefore, the approximation of no diffusion for colloids will result in predictions that underestimate repository performance. In TSPA-LA runs, colloid facilitated radionuclide transport is investigated through the FEHM colloid transport model and variations of colloid transport parameters.

Supporting Reports: *Conceptual Model and Numerical Approaches for UZ Flow and Transport* (BSC 2004 [DIRS 170035]); *Particle Tracking Model and Abstraction of Transport Processes* (BSC 2004 [DIRS 170041]); *Saturated Zone Colloid Transport* (BSC 2004 [DIRS 170006])

6.2.32 Chemistry of Water Flowing into the Drift (2.2.08.12.0A)

FEP Description: Inflowing water chemistry may be used in analysis or modeling that requires initial water chemistry in the drift. Chemistry of water flowing into the drift is affected by initial water chemistry in the rock, mineral and gas composition in the rock, and thermal-hydrologic-chemical processes in the rock.

Screening Decision: Included.

TSPA Disposition: The THC seepage model was designed specifically to investigate the effect of thermal-hydrologic-chemical processes in the host rock (BSC 2004 [DIRS 172463], Section 6.2.1.2), including the effects of initial water chemistry (BSC 2004 [DIRS 172463], Section 6.2.2.1), and mineral and gas compositions in the rock (BSC 2004 [DIRS 172463], Section 6.2.2.2). Therefore, these effects are explicitly accounted for in the results from the THC seepage model, and their abstraction in *Post-Processing Analysis for THC Seepage* (BSC 2004 [DIRS 169858], Section 6.2). Summary tables of concentrations through time are presented in DTNs: LB0302DSCPTHCS.002 [DIRS 161976], LB0307DSTTHCR2.002 [DIRS 165541], and summary statistics through time are presented in LB0311ABSTHCR2.001 [DIRS 166714]. These data are used to feed and/or provide technical basis for *Engineered Barrier System*:

Physical and Chemical Environment Model (BSC 2004 [DIRS 169860]), which generates look-up tables used in the TSPA-LA model. Because in the analysis of seepage water chemistry no water is predicted to actually seep into the modeled drift, the abstraction method was specifically designed to consider waters deemed most representative of potential in-drift seepage (BSC 2004 [DIRS 169858], Section 6.2.1; DTN: LB0311ABSTHCR2.001 [DIRS 166714]). The evaluation of seepage flow rates into the drifts is discussed in FEP 2.2.07.20.0A.

Supporting Reports: *Drift-Scale THC Seepage Model* (BSC 2004 [DIRS 172463]); *Post-Processing Analysis for THC Seepage* (BSC 2004 [DIRS 169858]).

6.2.33 Microbial Activity in the UZ (2.2.09.01.0B)

FEP Description: Microbial activity in the UZ may affect radionuclide mobility in rock and soil through colloidal processes, by influencing the availability of complexing agents, or by influencing groundwater chemistry. Changes in microbial activity could be caused by the response of the soil zone to changes in climate.

Screening Decision: Included.

TSPA Disposition: The effects of microbes on sorption are included in the distributions for sorption coefficients used in TSPA-LA. The sorption coefficient data on which the distributions are based are obtained in laboratory experiments in which crushed rock samples from the Yucca Mountain site are contacted with groundwaters (or simulated groundwaters) representative of the site, spiked with one or more of the elements of interest (BSC 2004 [DIRS 164500], Section A5). These K_d values, which include the effects of microbial activity, are used in *Particle Tracking Model and Abstraction of Transport Processes* (BSC 2004 [DIRS 170041], Section 6.5.4).

The basic technique for the laboratory determination of sorption coefficients involved the contact of a groundwater sample, spiked with the radionuclide of interest, with a crushed sample of tuff or alluvium. The rock sample was generally obtained as a core sample. The rock and water samples were not sterilized and, therefore, contain representative microbial biota from the UZ. Sorption experiments have been carried out as a function of time, element concentration, atmospheric composition, particle size, and temperature. In some cases, the solids remaining from sorption experiments were contacted with unspiked groundwater in desorption experiments. The effects of microbial activity with respect to sorption coefficients are provided in terms of probability distributions for the sorption coefficient of each element of interest among the three major rock types (devitrified, zeolitic, and vitric) found in the UZ. The influence of expected variations in water chemistry, radionuclide concentrations, and variations in rock surface properties within one of the major rock types are incorporated into these probability distributions. These distributions are specified for each radionuclide-rock type combination (BSC 2004 [DIRS 164500], Section A8) and are sampled in the TSPA-LA to account for the effects of natural variations in porewater chemistry and mineral surfaces on sorption. Correlations for sampling sorption coefficient probability distributions have been derived for the elements BSC 2004 [DIRS 164500], Appendix B).

Supporting Reports: *Particle Tracking Model and Abstraction of Transport Processes* (BSC 2004 [DIRS 170041]); *Radionuclide Transport Models Under Ambient Conditions* (BSC 2004 [DIRS 164500]).

6.2.34 Natural Geothermal Effects on Flow in the UZ (2.2.10.03.0B)

FEP Description: The existing geothermal gradient, and spatial or temporal variability in that gradient, may affect groundwater flow in the UZ.

Screening Decision: Included.

TSPA Disposition: Natural geothermal effects are included in the models of thermal-hydrologic processes used to describe the effects of waste heat in the repository (BSC 2004 [DIRS 169866]) The initial and boundary temperature conditions represent the natural geothermal gradient (BSC 2004 [DIRS 169866], Section 6.1.3). This temperature profile is primarily determined by the ground surface temperature, the water table temperature, water flux through the UZ, and the thermal conductivity from layer to layer. Natural geothermal effects on unsaturated flow in the absence of repository thermal effects have been investigated in the models of natural thermal processes in the UZ (BSC 2004 [DIRS 169861], Section 6.3). The results of these models indicate that the effects of the natural temperature gradient on UZ flow are insignificant.

The natural geothermal gradient at Yucca Mountain is explicitly included in starting conditions of the TH seepage model in *Drift-Scale Coupled Processes (DST and TH Seepage) Models* (BSC 2004 [DIRS 170338]) and thereby included in *Abstraction of Drift Seepage* (BSC 2004 [DIRS 169131], Section 6.4.3). The natural geothermal gradient is also included in the THC seepage model in *Drift-Scale THC Seepage Model* (BSC 2004 [DIRS 172463]), and in the abstraction of drift seepage (BSC 2004 [DIRS 169131], Section 6.4.4) by setting the ground surface temperature (top model boundary) and the temperature at the water table (bottom boundary) to measured values (BSC 2004 [DIRS 172463], Section 6.5.2). The effect of this temperature gradient on flow is explicitly accounted for by the coupled heat-flow transport algorithms implemented in the THC simulator (TOUGHREACT V3.0 LBNL 2002 [DIRS 161256]). Therefore, this effect is explicitly taken into account in the results of the THC seepage model; summary tables of concentrations through time submitted under DTNs: LB0302DSCPTHCS.002 [DIRS 161976], LB0307DSTTHCR2.002 [DIRS 165541], and tables of concentrations and summary statistics through time submitted under DTN: LB0311ABSTHCR2.001 [DIRS 166714]. DTNs: LB0302DSCPTHCS.002 [DIRS 161976] and LB0311ABSTHCR2.001 [DIRS 166714] are used to feed and/or provide technical basis for *Engineered Barrier System: Physical and Chemical Environment Model* (BSC 2004 [DIRS 169860]), which generates look-up tables used in the TSPA-LA model.

Natural geothermal effects on unsaturated flow in the absence of repository thermal effects have been investigated in the models of natural thermal processes in the UZ (BSC 2004 [DIRS 169861], Section 6.3). The results of these models have found indicate that the effects of the natural temperature gradient on UZ flow are insignificant.

Supporting Reports: *Drift-Scale THC Seepage Model* (BSC 2004 [DIRS 172463]); *Abstraction of Drift Seepage* (BSC 2004 [DIRS 169131]); *Drift-Scale Coupled Processes (DST and TH*

Seepage) Models (BSC 2004 [DIRS 170338]); *UZ Flow Models and Submodels* (BSC 2004 [DIRS 169861]).

6.2.35 Two-Phase Buoyant Flow/Heat Pipes (2.2.10.10.0A)

FEP Description: Heat from waste can generate two-phase buoyant flow. The vapor phase (water vapor) could escape from the mountain. A heat pipe consists of a system for transferring energy between a hot and a cold region (source and sink respectively) using the heat of vaporization and movement of the vapor as the transfer mechanism. Two-phase circulation continues until the heat source is too weak to provide the thermal gradients required to drive it. Alteration of the rock adjacent to the drift may include dissolution that maintains the permeability necessary to support the circulation (as inferred for some geothermal systems).

Screening Decision: Included.

TSPA Disposition: The coupled processes causing heat-pipe behavior (BSC 2004 [DIRS 169131], Section 6.3.2) are explicitly simulated with the TH seepage model (BSC 2004 [DIRS 170338]) that feeds into the seepage abstraction. Using this model, the impact of heat-pipe behavior on seepage is assessed for various simulation cases (BSC 2004 [DIRS 169131], Section 6.4.3.3). Thus, the TH-modeling results from DTN: LB0301DSCPTHSM.002 [DIRS 163689] inherently include the effect of heat pipes. As discussed in *Abstraction of Drift Seepage* (BSC 2004 [DIRS 169131], Section 6.5.2), the abstraction of thermal seepage utilizes these modeling results to develop an appropriate thermal-seepage abstraction methodology.

The coupled processes causing heat-pipe behavior are explicitly simulated with the THC seepage model (BSC 2004 [DIRS 172463], Section 6.2.1.1). The continuous boiling and refluxing of water in this zone affects water-rock interactions (BSC 2004 [DIRS 172463], Section 6.2.1.2). The resulting water chemistry in the heat pipe is captured by the HISAT waters (BSC 2004 [DIRS 169858], Section 6.2.3; BSC 2004 [DIRS 172463], Section 6.5.5.2.2). Therefore, the effect of heat pipes on predicted water and gas chemistries is explicitly taken into account in the results of the THC seepage model and their abstraction (BSC 2004 [DIRS 169858], Section 6.2; summary tables of concentrations through time submitted under DTNs: LB0302DSCPTHCS.002 [DIRS 161976], LB0307DSTTHCR2.002 [DIRS 165541]; and tables of concentrations and summary statistics through time submitted under DTN: LB0311ABSTHCR2.001 [DIRS 166714]). DTNs: LB0302DSCPTHCS.002 [DIRS 161976] and LB0311ABSTHCR2.001 [DIRS 166714] are used to feed and/or provide technical basis for *Engineered Barrier System: Physical and Chemical Environment Model* (BSC 2004 [DIRS 169860]), which generates look-up tables used in the TSPA-LA model.

Supporting Reports: *Drift-Scale THC Seepage Model* (BSC 2004 [DIRS 172463]); *Abstraction of Drift Seepage* (BSC 2004 [DIRS 169131]); *Drift-Scale Coupled Processes (DST and TH Seepage) Models* (BSC 2004 [DIRS 170338]).

6.2.36 Geosphere Dry-Out due to Waste Heat (2.2.10.12.0A)

FEP Description: Repository heat evaporates water from the UZ rocks near the drifts as the temperature exceeds the vaporization temperature. This zone of reduced water content (reduced

saturation) migrates outward during the heating phase (about the first 1000 years) and then migrates back to the waste packages as heat diffuses throughout the mountain and the radioactive sources decay. This FEP addresses the effects of dry-out within the rocks.

Screening Decision: Included.

TSPA Disposition: The coupled processes of vaporization, dryout, and resaturation are explicitly simulated with the TH seepage model (BSC 2004 [DIRS 170338]) that feeds into the seepage abstraction. Using this model, the impact of such coupled processes on seepage is assessed for various simulation cases (BSC 2004 [DIRS 169131], Section 6.4.3.3). Thus, the TH-modeling results from DTN: LB0301DSCPTHSM.002 [DIRS 163689] inherently include these effects. As discussed in *Abstraction of Drift Seepage* (BSC 2004 [DIRS 169131], Section 6.5.2), the abstraction of thermal seepage utilizes these modeling results to develop an appropriate thermal-seepage abstraction methodology.

The coupled processes of vaporization, dryout, and resaturation are explicitly simulated with the THC seepage model, including the formation of a dry (or nearly dry) zone around drifts, expanding and then receding through time following the pulse of heat released from the waste packages (BSC 2004 [DIRS 172463], Sections 6.2.1 and 6.5.5.1). Therefore, these effects are explicitly accounted for in the results from the THC seepage model, and in their abstraction in *Post-Processing Analysis for THC Seepage* (BSC 2004 [DIRS 169858], Section 6.2). Summary tables of concentrations through time are presented in DTNs: LB0302DSCPTHCS.002 [DIRS 161976], LB0307DSTTHCR2.002 [DIRS 165541], and summary statistics through time are presented in LB0311ABSTHCR2.001 [DIRS 166714]. These data are used to feed and/or provide technical basis for *Engineered Barrier System: Physical and Chemical Environment Model* (BSC 2004 [DIRS 169860]), which generates look-up tables used in the TSPA-LA model. The effects of dryout on surface infiltration are discussed in FEP 2.2.10.01.0A.

Supporting Reports: *Drift-Scale THC Seepage Model* (BSC 2004 [DIRS 172463]); *Abstraction of Drift Seepage* (BSC 2004 [DIRS 169131]); *Drift-Scale Coupled Processes (DST and TH Seepage) Models* (BSC 2004 [DIRS 170338]).

6.2.37 Topography and Morphology (2.3.01.00.0A)

FEP Description: This FEP is related to the topography and surface morphology of the disposal region. Topographical features include outcrops and hills, water-filled depressions, wetlands, recharge areas and discharge areas. Topography, precipitation, and surficial permeability distribution in the system will determine the flow boundary conditions (i.e., location and amount of recharge and discharge in the system).

Screening Decision: Included.

[DIRS 165991], Table 6-3 and Section 6.1.2.). The evapotranspiration-rate multiplier POTETMUL operates on the evapotranspiration rate, as calculated within the infiltration model software, INFIL VA_2.a1 (SNL 2001 [DIRS 147608]) (and also INFIL V2.0; USGS 2001 [DIRS 139422]). Surface runoff is incorporated through the inclusion of a parameter (FLAREA) that defines the fraction of each grid cell in the infiltration model that is affected by overland flow and channel flow during the routing of runoff. It is incorporated implicitly by inclusion of uncertainty in the fraction of each grid cell in the infiltration model that is affected by overland flow and channel flow during the routing of runoff in the calculation of the weighting factors that are passed to TSPA-LA (BSC 2003 [DIRS 165991] and DTN: SN0308T0503100.008 [DIRS 165640]).

Supporting Reports: *Simulation of Net Infiltration for Present-Day and Potential Future Climates* (BSC 2004 [DIRS 170007]); *Analysis of Infiltration Uncertainty* (BSC 2003 [DIRS 165991]); *UZ Flow Models and Submodels* (BSC 2004 [DIRS 169861]).

6.2.40 Infiltration and Recharge (2.3.11.03.0A)

FEP Description: Infiltration into the subsurface provides a boundary condition for groundwater flow. The amount and location of the infiltration influences the hydraulic gradient and the height of the water table. Different sources of recharge water could change the composition of groundwater passing through the repository. Mixing of these waters with other groundwaters could result in precipitation, dissolution, and altered chemical gradients.

Screening Decision: Included.

TSPA Disposition: The hydrological effects of infiltration and recharge are included in the infiltration model (FEP 1.3.01.00.0A). This model includes the effects of seasonal and climate variations, climate change, surface-water runoff, and site topography such as hillslopes and washes to simulate the spatial distribution of infiltration as described in *Simulation of Net Infiltration for Present-Day and Potential Future Climates* (BSC 2004 [DIRS 170007], Section 6.11). The time dependence of infiltration results is linked to the timing of climate change as discussed in Section 6.2.4; FEP 1.3.01.00.0A. This is incorporated into the TSPA-LA through the UZ flow fields that use the infiltration model results (DTN: GS000308311221.005 [DIRS 147613]) as upper boundary conditions (BSC 2004 [DIRS 169861], Section 6.1.4). Flow fields for TSPA-LA are in DTN: LB0305TSPA18FF.001 [DIRS 165625]. Data for calibrating the infiltration model were acquired in experiments at Alcove 1, as reported in *In Situ Field Testing of Processes* (BSC 2004 [DIRS 170004], Section 6.12).

The effects of present-day water composition infiltrating from the ground surface are accounted for in the analysis of seepage-water chemistry by using the measured porewater chemistry in the UZ (BSC 2004 [DIRS 172463], Table 6.2-1). However, porewater chemistry varies by hydrologic unit (BSC 2004 [DIRS 172463], Figure 6.2-4). Variation in the quality of infiltrating water is dominated by rock–water interaction.

Infiltration uncertainty, as it applies to the determination of weighting factors used in TSPA-LA (DTN: SN0308T0503100.008 [DIRS 165640]), is documented in *Analysis of Infiltration Uncertainty* (BSC 2003 [DIRS 165991]). The way it is handled is summarized in *Analysis of Infiltration Uncertainty* (BSC 2003 [DIRS 165991], Section 1.1). TSPA-LA has included three

movement to the waste emplacement drifts or radionuclide transport from the waste emplacement drifts to the water table. Table 6-4 lists 8 deep boreholes in the repository block and 7 deep boreholes near the repository block. The definition for deep borehole in the repository block is a borehole that penetrates the TSw. The definition for deep borehole near the repository block is a borehole that penetrates below the elevation of waste emplacement (DTNs: MO9906GPS98410.000 [DIRS 109059], MO0004QGFMPIK.000 [DIRS 152554], and *D&E/PA/C IED Subsurface Facilities* (BSC 2004 [DIRS 164519])). Boreholes that terminate in or above the PTn will have a negligible effect on percolation flux at the repository because flow through these boreholes will tend to be homogenized by matrix flow in the underlying Paintbrush nonwelded hydrogeologic unit (*UZ Flow Models and Submodels*, BSC 2004 [DIRS 169861], Appendix G; CRWMS M&O 1998 [DIRS 100356], Section 2.4.2.8; Wu et al. 2000 [DIRS 154918], Section 4.1). The locations of the boreholes listed in Table 6-4 relative to waste emplacement locations are shown in *D&E/PA/C IED Subsurface Facilities* (BSC 2004 [DIRS 168180]).

Many of the boreholes penetrate the UZ entirely and terminate at or below the water table. Based on the design layout (BSC 2004 [DIRS 164519]) and borehole locations in Table 6-4, none of the existing boreholes will intersect with a waste emplacement drift. Therefore, water entering these boreholes would continue to flow through these boreholes to the water table, bypassing waste emplacement locations. One of the deep boreholes within the waste emplacement footprint, USW UZ-1, only partially penetrates the UZ. USW UZ-1 has a total depth of 1,270 ft, but terminates near the TSw vitrophyre beneath waste emplacement locations. Therefore, none of the deep boreholes in the repository block terminates above potential waste emplacement locations. In the event that a drift unexpectedly encounters a borehole during repository construction, such boreholes will either be sealed or waste packages will have a stand-off distance from the location of the borehole penetration into the waste emplacement drift, or both.

The other aspect of this problem is the movement of dissolved radionuclides and radionuclides associated with mobile colloids between the repository and the water table. Fractures and faults represent continuous rapid-transport pathways from the repository to the water table. Any significant lateral flow beneath the repository eventually finds one of these high-permeability pathways to the water table. The principal difference between these high-permeability pathways and boreholes is that the cross-sectional area of the boreholes available to intercept lateral flow is much smaller than the area associated with fractures and faults. The 15 boreholes in Table 6-4 with depths greater than 1,000 ft present a total cylindrical area (available to intercept lateral flow) per unit depth that may be calculated by the product of the borehole diameter times the number of boreholes. The average borehole diameter is bounded by a value of 1 m (Table 6-4), given that borehole diameters can exceed the size of the drill bit. This gives a total borehole sidewall area per unit depth of $15\pi \text{ m}^2/\text{m}$. The fractured rock between the repository and the water table has a fracture area per unit volume of 0.1 m^{-1} or more (BSC 2004 [DIRS 170038], Table 6-5). Multiplying this by the $5 \times 10^6 \text{ m}^2$ footprint of the repository (BSC 2004 [DIRS 168370]) gives a minimum fracture area per unit depth of about $5 \times 10^5 \text{ m}^2/\text{m}$. Therefore, the contribution of boreholes to the steady state flow and transport pattern between the repository and the water table is negligible. A potential scenario that could lead to greater radionuclide releases is the migration of perched water through the borehole pathways if a borehole seal should fail.

6.4.5 Flow in the UZ from Episodic Infiltration (2.2.07.05.0A)

FEP Description: Episodic flow could occur in the UZ as a result of episodic infiltration. Episodic flow may affect radionuclide transport.

Screening Decision: Excluded–Low Consequence.

Screening Argument: The process that drives infiltration in the UZ is precipitation, which is clearly episodic in nature. Studies of episodic infiltration and percolation have found, however, that matrix-dominated flow in the Paintbrush Tuff nonwelded hydrogeologic unit (PTn) damps out the transient nature of the percolation such that UZ flow below the PTn is essentially steady (BSC 2004 [DIRS 169861], Appendix G).

The PTn primarily consists of nonwelded to partially welded tuffs and extends from the base of the densely to moderately welded Tiva Canyon welded tuff (TCw) to the top of the densely welded Topopah Spring welded (TSw) hydrogeologic unit. Within the repository area, the thickness of the PTn unit ranges from approximately 30 to 60 m. As a whole, the PTn unit exhibits different hydrogeologic properties than the TCw and TSw units that bound it above and below. Both the TCw and the TSw units display the low porosity and intense fracturing typical of the densely welded tuffs at Yucca Mountain. In contrast, with its high porosity and low fracture intensity, the matrix of the PTn has a large capacity for storing groundwater and effectively damps percolation flux at the base of the TCw unit. Water imbibing into the PTn matrix from rapid fracture flow of the TCw results in a more uniform distribution of flux at the base of the PTn after traveling through the entire PTn unit.

Calculations with infiltration boundary conditions of 5 mm/yr and 20 mm/yr (BSC 2004 [DIRS 169861], Figures G-11 and G-12) show the flow damping effect. This conclusion is supported by additional calculations (Wu et al. 2000 [DIRS 154918], Section 4.1; Wu et al. 2002 [DIRS 161058]). Furthermore, the PTn overlies the entire repository block (Appendix B). This damping of transient flow is due to capillary forces and high matrix permeability in the PTn that lead to matrix imbibition of water from fractures to the matrix. This is also supported by carbon-14 data collected in bedded tuffs of the PTn unit (BSC 2004 [DIRS 169861], Appendix G) as well as by results of a water-release test at Alcove 4 and the results of line surveys of fracture minerals in the ESF and ECRB Cross-Drift (BSC 2004 [DIRS 170004], Sections 6.7 and 6.14.1). Therefore, this FEP is excluded on the basis that the UZ flow is steady at the repository and along radionuclide transport pathways.

Very small amounts of fracture flow do appear to penetrate as fast pathways through fault zones between the ground surface and the repository elevation as evidenced by high ^{36}Cl concentrations in samples taken from the Exploratory Studies Facility (ESF). Higher concentrations of this isotope found in the ESF can only be explained through surface deposition of ^{36}Cl from nuclear weapons testing and subsequent aqueous transport to certain ESF sampling locations in a period of approximately 50 years. The flow responsible for rapid transport could occur either as steady flow or as episodic transient flow. In either case, the key to fast transport through the PTn is for solute to move through fractures and bypass transport through the rock matrix. However, the flow and transport models indicate that the quantity of water and dissolved constituents that do penetrate the PTn as a result of fast pathways (generally less than 1 percent

relative to gas pressure effects. This can be seen by comparing the gas-phase pressures in fractures for TH calculations (no mineral precipitation) with those for THC calculations (mineral precipitation included) (DTN: LB0302DSCPTHCS.002 [DIRS 161976]; BSC 2004 [DIRS 172463]). These analyses include the effects the phase change of water to vapor under the higher temperatures caused by waste heat from the repository. This FEP also addresses the effects of gas bubbles. Because the repository at Yucca Mountain is located in the UZ with high aqueous to gas-phase contact, bubbles would quickly be absorbed into the gas phase and could not drive substantial water flow. Therefore, the bubble-release mechanism is negligible. This argument is valid regardless of the specific potential sources of gas generation (e.g., degradation of repository components or microbial degradation of organic matter). This FEP is, therefore, excluded because it will not significantly change radiological exposures to the RMEI or radiological releases to the accessible environment. Section 6.1.2 explains why low consequence for specific elements of the UZ system leads to low consequence for total system performance.

Supporting Reports: Not applicable.

6.7.3 Gas Transport in Geosphere (2.2.11.03.0A)

FEP Description: Gas released from the drifts and gas generated in the near-field rock will flow through fracture systems in the near-field rock and in the geosphere. Certain gaseous or volatile radionuclides may be able to migrate through the far-field faster than the groundwater advection rate.

Screening Decision: Excluded–Low Consequence.

Screening Argument: All radionuclides in the nominal scenario for TSPA-LA are transported from the repository to the accessible environment into the aqueous phase (DOE 2002 [DIRS 155970], Section I.7). This is expected to bound any dose effects of gas-phase transport in the geosphere. The only radionuclides that would have a potential for gas transport are ^{14}C and ^{222}Rn . ^{129}I can exist in a gas phase, but it is highly soluble and, therefore, would be more likely to dissolve in groundwater rather than migrate as a gas. Other gas-phase isotopes have been eliminated in a screening analysis (DOE 2002 [DIRS 155970], Section I.3.3), usually because they have short half-lives and are not decay products of long-lived isotopes. Note that for ^{14}C and ^{222}Rn , the process of inhalation dose in the biosphere model is included (BSC 2004 [DIRS 169826], Section 6.2.45)

An analysis of the potential dose from gas-phase geosphere transport of carbon-14 shows that the individual maximum radiological dose rate was found to be 1.8×10^{-10} mrem per year (DOE 2002 [DIRS 155970], Section I.7). This may be compared with doses from ^{14}C in *Total System Performance Assessment for the Site Recommendation* (TSPA-SR) CRWMS M&O 2000 [DIRS 153246], Figure 4.1-7), which found peak doses from aqueous ^{14}C release to be in excess of 10^{-4} mrem/yr. Because gas-phase releases comprise approximately 2 percent of the ^{14}C inventory (DOE 2002 [DIRS 155970], Section I.7), this fraction should result in a maximum dose rate of about 10^{-6} mrem/yr, given aqueous release. Therefore, the dose from aqueous geosphere transport of carbon-14 bounds the dose from gas-phase geosphere transport pathways.

to less than 100 years and alteration limited to zones of a few meters around the dike, the thermal and chemical effects of basaltic magmatism on UZ processes is negligible. The effects on water level are discussed in Section 6.8.3 (FEP 1.2.10.01.0A).

Igneous activity could also affect the ground surface of the repository through eruptions of lava or ash. If lava were to dam one or more washes that drain the repository block, the dam would not produce a large surface-water impoundment relative to the repository emplacement area. Such lava dams would probably not be effective in any case, as the lava would consist of clinker or aa (aa is a lava flow with a surface typified by angular, jagged blocks). Another potential effect would be the deposition of an ash cover on the repository block. The median grain size of ash deposits investigated at the Lathrop Wells cone ranged from 0.18 to 2.8 mm (BSC 2004 [DIRS 169980], Table C-7). This grain size is characteristic of a medium to coarse sand, which has a typical porosity range of 0.35 to 0.4 (Bear 1972 [DIRS 156269], pp. 40 and 46). Using these porosity and grain size ranges and the modified Kozeny-Carmen equation for permeability (Bear 1972 [DIRS 156269], p. 166):

$$k = \frac{d_m^2}{180} \frac{n^3}{(1-n)^2} \quad (\text{Eq. 6-2})$$

where k is permeability, d_m is grain size, and n is porosity, the estimated permeability range of the ash deposit is 2×10^{-11} to $8 \times 10^{-9} \text{ m}^2$. Bedrock permeability in the infiltration model ranges from 1×10^{-17} to $6 \times 10^{-13} \text{ m}^2$ and soil permeability ranges from 6×10^{-13} to $4 \times 10^{-12} \text{ m}^2$ (BSC 2004 [DIRS 170007], Appendix B). Therefore, an ash deposit is expected to be orders of magnitude more permeable than the underlying bedrock and soil. Rainfall will tend to infiltrate and run off along the ash-bedrock or ash-soil interface resulting in minimal effects of the ash on runoff or infiltration.

As an additional consideration, the mean probability for the occurrence of a volcanic intrusion at Yucca Mountain is 1.7×10^{-8} per year (BSC 2004 [DIRS 169989], Table 7-1). This results in a greatly reduced expected consequence from a probability-weighted perspective. This FEP is, therefore, excluded because it will not significantly change radiological exposures to the RMEI or radiological releases to the accessible environment. Section 6.1.2 explains why low consequence for specific elements of the UZ system leads to low consequence for total system performance.

Supporting Reports: Not applicable.

6.8.5 Seismic Activity Changes Porosity and Permeability of Rock (2.2.06.01.0A)

FEP Description: Seismic activity (fault displacement or vibratory ground motion) has a potential to change rock stresses and result in strains that affect flow properties in rock outside the excavation-disturbed zone. It could result in strains that alter the permeability in the rock matrix. These effects may decrease the transport times for potentially released radionuclides.

Screening Decision: Excluded–Low Consequence.

Screening Argument: The thermal-chemical interactions that will occur in the repository environment have been studied with respect to effects on the seepage water entering the waste emplacement drifts using the THC seepage model (BSC 2004 [DIRS 172463]). This model, which explicitly captures the effects of changes in temperature, pH, Eh, ionic strength (and other compositional variables), time dependency, precipitation or dissolution effects, and effects of resaturation, was used to examine near-field and drift seepage flow and chemistry (BSC 2004 [DIRS 172463], Section 6.2). Changes in fracture permeabilities were found to be on the order of the natural variation in these properties (BSC 2004 [DIRS 172463], Section 6.5.5.3; BSC 2004 [DIRS 170038], Table 6-5), with most of the substantial effects limited to regions above and to the side of the drift within about a drift diameter (BSC 2004 [DIRS 172463], Figures 6.5-39 and 6.5-40). The predicted mineral precipitation reduces permeability in the affected regions and leads to a reduction in flow around the drift. Likewise, any mineralogical changes are of very limited extent below the drift, resulting in negligible effects on radionuclide sorption (BSC 2004 [DIRS 169866], Section 6.4.3.3.3). THC effects on fracture characteristics have been evaluated with process models that explicitly account for fracture flow affected by THC parameter alterations (BSC 2004 [DIRS 169131], Section 6.4.4.2). It was demonstrated that the effects of these potential alterations on near-field and drift seepage flow can be neglected in the TSPA-LA, because the expected changes would lead to less seepage (BSC 2004 [DIRS 169131], Section 6.5.1.4). Consequently, neglect of this effect is likely to result in slightly conservative model predictions for both drift seepage and radionuclide transport phenomena. Therefore, this FEP is excluded because it will have no adverse effects on the radiological exposures to the RMEI, or radionuclide release to the accessible environment. Section 6.1.2 explains why low consequence for specific elements of the UZ system leads to low consequence for total system performance.

Note that the THC effects (e.g., mineral precipitation) on fracture characteristics as they relate to near-field and drift seepage chemistry were also evaluated with the THC seepage model. A discussion is provided in FEP 2.2.03.02.0A.

Supporting Reports: Not applicable.

6.9.2 Chemical Effects of Excavation and Construction in the Near-Field (2.2.01.01.0B)

FEP Description: Excavation may result in chemical changes to the incoming groundwater and to the rock in the excavation disturbed zone.

Screening Decision: Excluded–Low Consequence.

Screening Argument: This FEP concerns the changes in the host rock environment immediately surrounding the waste emplacement drifts. Related FEP 1.1.02.00.0A (Chemical effects of excavation and construction in the EBS) is discussed in *Engineered Barrier System Features, Events, and Processes* (BSC 2004 [DIRS 169898], Section 6.2.1). Changes are expected in the rock fracture properties from excavation disturbance, stress relief around the opening, and ground support. However, these changes will not affect water chemistry. Excavation will introduce water (for dust control), but this should not have any significant effect on water chemistry. This is based on the limited volumes of water that are typically lost during underground excavation (for example, for ESF construction the average was required to be less

it will have no adverse affects on the radiological exposures to the RMEI, or radionuclide release to the accessible environment. Section 6.1.2 explains why low consequence for specific elements of the UZ system leads to low consequence for total system performance.

Supporting Reports: Not applicable.

6.9.4 Changes in Fluid Saturations in the Excavation Disturbed Zone (2.2.01.03.0A)

FEP Description: Fluid flow in the region near the repository may be affected by the presence of the excavation, waste, and EBS. Some dry-out will occur during excavation and operations.

Screening Decision: Excluded–Low Consequence.

Screening Argument: Inclusion of preclosure dryout is not significant for thermal seepage (BSC 2004 [DIRS 170338], Section 6.2.1.3.3). The overall effect of ventilation dryout on drift-scale radionuclide transport may also be excluded, because thermal dryout and rewetting will erase nearly any effect of the ventilation dryout. Sensitivity studies in *FY 01 Supplemental Science and Performance Analyses, Volume 1: Scientific Bases and Analyses* (BSC 2001 [DIRS 155950], Section 5.3.2.4.4) indicate that inclusion of preclosure dryout gives rise to slightly higher temperatures during the heating period compared to a model that ignores the influence of preclosure dryout. Therefore, this FEP may be excluded based on low consequence. Section 6.1.2 explains why low consequence for specific elements of the UZ system leads to low consequence for total system performance.

Other aspects of this FEP are discussed elsewhere. For the effects of the excavation on fluid flow, see FEP 2.2.07.20.0A; for the effects of waste heat on fluid flow, see FEPs 2.2.10.10.0A and 2.2.10.12.0A; for the effects of the EBS (rock bolt holes) on fluid flow, see FEP 1.1.01.01.0B.

Supporting Reports: Not applicable.

6.9.5 Radionuclide Solubility in the Excavation Disturbed Zone (2.2.01.04.0A)

FEP Description: Radionuclide solubility limits in the excavation-disturbed zone may differ from those in the EBS.

Screening Decision: Excluded–Low Consequence.

Screening Argument: If solubility limits are lower in the EDZ than in the emplacement drifts, then some dissolved radionuclides will precipitate as water flows out of the drifts. In this case, exclusion of the FEP would not result in an underestimation of radionuclide transport. The magnitude of this conservative approximation may be qualitatively evaluated through a comparison of the different ranges of chemical environments estimated for the engineered barrier system as compared with the EDZ and UZ in general. The pH of waters inside the drift range from less than 5 to more than 10 (BSC 2004 [DIRS 169860], Figures 6.13-2 through 6.13-12). The evolution of water chemistry in the UZ, however, is not so broad. Near the drift the pH ranges from roughly 7 to 8.5 (BSC 2004 [DIRS 172463], Figures 6.5-12, 6.5-25, 6.5-58). Further out into the rock, the pH ranges from about 7 to 9 (BSC 2004 [DIRS 169866],

and 6.6.1). Therefore, the limited extent of the EDZ compared with the overall transport path length in the UZ (approximately 300 m) also leads to the conclusion that the effects of the EDZ is negligible for colloid and radionuclide transport. Therefore, the effects of altered fracture properties in the EDZ are excluded because they will not significantly change radiological exposures to the RMEI or radiological releases to the accessible environment. Section 6.1.2 explains why low consequence for specific elements of the UZ system leads to low consequence for total system performance.

The effects of precipitation of aqueous radionuclides on transport in the EDZ also are excluded (FEP 2.2.01.04.0A). Excluding precipitation for radionuclides that undergo simple decay is conservative because this can only enhance the radionuclide mass flux at the accessible environment. For radionuclides that undergo chain decay, excluding precipitation will be conservative because the radionuclide source is not significantly depleted within the 10,000-year regulatory time period. In the latest total-system performance assessment, dose rates for all radionuclides are predicted to increase over tens of thousands of years (CRWMS M&O 2000 [DIRS 153246], Figures 4.1-5 and 4.1-7). This is a result of the spread of waste package failures over time (CRWMS M&O 2000 [DIRS 153246], Figure 4.1-9) and the slow release of radionuclides from the waste emplacement drifts. Therefore, during the 10,000-year period, the highest concentration for any radionuclide at the receptor is expected to occur under conditions giving the greatest transport rates. Reduced solubilities for neptunium, americium, plutonium, thorium, and uranium were investigated as a sensitivity in TSPA-SR (CRWMS M&O 2000 [DIRS 153246], Sections 3.5.5, 4.1.3, and Figures 4.1-19a and 4.1-20). The dose rates for radionuclides affected by the lower solubilities (including decay products such as ^{226}Ra) were found to be lower in the reduced-solubility case. This leads to the conclusion that suppressing precipitation of radionuclides in the TSPA-LA model results in higher calculated dose rates. Therefore, precipitation of radionuclides is excluded; this exclusion leads to underestimation of repository performance.

The principal effects of the near-field environment on transport are temperature and geochemical environment. Thermal effects on sorption are evaluated in Section 6.9.13 (FEP 2.2.10.06.0A), where increased temperatures are found to lead to increased sorption. Compositional variations found at the base of the drift in *Drift-Scale THC Seepage Model* (BSC 2004 [DIRS 172463], Figures 6.5-12 to 6.5-20) lie within the range of compositional variations expected in the unsaturated zone and accounted for in terms of radionuclide sorption (BSC 2004 [DIRS 164500], Section A4).

Supporting Reports: Not applicable.

6.9.7 Geochemical Interactions and Evolution in the UZ (2.2.08.03.0B)

FEP Description: Groundwater chemistry and other characteristics, including temperature, pH, Eh, ionic strength, and major ionic concentrations, may change through time, as a result of the evolution of the disposal system or from mixing with other waters. Geochemical interactions may lead to dissolution and precipitation of minerals along the groundwater flow path, affecting groundwater flow, rock properties, and sorption of radionuclides. Effects on hydrologic flow properties of the rock, radionuclide solubilities, sorption processes, and colloidal transport are

relevant. Kinetics of chemical reactions should be considered in the context of the time scale of concern.

Screening Decision: Excluded–Low Consequence.

Screening Argument: The thermal-chemical interactions that will occur in the repository environment have been studied with respect to effects on the seepage water entering the waste emplacement drifts using the THC seepage model (BSC 2004 [DIRS 172463]). This model, which explicitly captures the effects of changes in temperature, pH, Eh, ionic strength (and other compositional variables), time dependency, precipitation or dissolution effects, and effects of resaturation, was used to examine near-field and drift seepage flow and chemistry (BSC 2004 [DIRS 172463], Section 6.2). Changes in fracture permeabilities were found to be on the order of the natural variation in these properties (BSC 2004 [DIRS 172463], Section 6.5.5.3 and BSC 2004 [DIRS 170038], Table 6-5), with most of the substantial effects limited to regions above and to the side of the drift within about a drift diameter (BSC 2004 [DIRS 172463], Figures 6.5-39, 6.5-40). The predicted mineral precipitation reduces the permeability in the affected regions, and leads to a reduction in flow around the drift. These effects may be excluded because including such changes in fracture permeability would result in lower predicted doses in TSPA. Note that the effects of mineral precipitation on fracture permeability as it relates to near-field and drift seepage chemistry was also evaluated with the THC seepage model. A discussion is provided in Section 6.2.11, FEP 2.2.03.02A.

The geochemical model includes the major solid phases (minerals and glass) encountered in geological units at Yucca Mountain, together with a range of possible reaction product minerals, CO₂ gas, and the aqueous species necessary to include these solid phases and the porewater composition within the THC model (BSC 2004 [DIRS 172463], Table 6.2-2). Compositional changes were only calculated near the drift boundary for the drift-scale THC seepage model (BSC 2004 [DIRS 172463]). Results from these simulations show most compositional variations returning to unperturbed conditions in 10,000 years or less. Variations in pH (BSC 2004 [DIRS 172463], Figures 6.5-12 and 6.5-25), a key compositional variable for sorption of some radionuclides (BSC 2004 [DIRS 164500], Appendix A), roughly lie within the range of variability investigated for initial porewater compositions (BSC 2004 [DIRS 172463], Table 6.2-1). Bicarbonate is found to be depressed in concentration upon water resaturation at the drift wall, as expected based on the reduced pH values for the same time period.

Results were also investigated for the Tptpll (lower lithophysal unit) model considering a range of initial porewater compositions. In this model, five different initial porewater compositions were investigated (BSC 2004 [DIRS 172463], Table 6.2-1). Peak concentrations usually found at the time of rewetting in both models reflect mostly the small values of the first nonzero liquid-saturation output. In any case, elevated concentrations are predicted only for small liquid saturations that are not subject to significant fluid movement. The improved treatment of mineral precipitation at the boiling front used in the most recent THC model for the Tptpll also results in the prediction of lower, more realistic aqueous silica concentrations than in earlier models (BSC 2004 [DIRS 172463], Figure 6.5-16). This model also predicts upon rewetting, more rapid return to near-ambient conditions for aqueous Ca, Na, and Cl.

The findings indicate that at the drift wall, most of the significant compositional variations resulting from thermal-chemical processes are limited to low-saturation conditions over time periods that are short relative to the 10,000-year performance period. Similar magnitudes of variation in chloride and pH were found in the mountain-scale THC model results (BSC 2004 [DIRS 169866], Section 6.4.3.3.2). The magnitudes of the variations are found to be smaller at greater distances from the drift wall. As for the drift-scale study, variations in chloride are driven mainly by evaporation and are found to return to near-ambient values upon rewetting (BSC 2004 [DIRS 169866], Section 6.4.3.3.2). Variations in pH were found to lie roughly between 7 and 9, which is similar to the results for the drift-scale THC model (BSC 2004 [DIRS 172463], Figures 6.5-12, 6.5-25 and 6.5-58). The most persistent change in pH is a level of about 7 in the Calico Hills, down from values between 7.5 and 8 (BSC 2004 [DIRS 169866], Section 6.4.3.3.2, Figure 6.4-17), but this lies within the range of pH investigated for radionuclide sorption (BSC 2004 [DIRS 164500], Appendix A). Therefore, the effects of these changes are excluded because they will not significantly change radiological exposures to the RMEI or radiological releases to the accessible environment. Section 6.1.2 explains why low consequence for specific elements of the UZ system leads to low consequence for total system performance.

Supporting Reports: Not applicable.

6.9.8 Radionuclide Solubility Limits in the UZ (2.2.08.07.0B)

FEP Description: Solubility limits for radionuclides may be different in unsaturated zone groundwater than in the water in the waste and EBS.

Screening Decision: Excluded—Low Consequence.

Screening Argument: In general the conditions that control the solubility of radionuclides will be different in the invert of the EBS and in the UZ, and may vary in the UZ with location and time. The conditions that control radionuclide solubility are identified in *Dissolved Concentration Limits of Radioactive Elements* (BSC 2004 [DIRS 169425]) and include pH, fugacity of CO₂, concentration of fluoride ion, and temperature. These variables are not all independent: at higher temperature, CO₂ gas is less soluble. This reduces the solubility of carbonate complexes, which at high pH are the species that contribute the most to actinide solubilities. The result is that actinides are less soluble at higher temperatures (BSC 2004 [DIRS 169425, Section 6.3.3.3, but note that only solubility limits at 25°C are used for TSPA). The drifts will be hotter than the UZ beneath the drifts at least for the first 8000 years (BSC 2004 [DIRS 169866], Figure 6.3.1-6). This suggests, therefore, that actinide solubility limits will be greater in the UZ than in the drift and will increase downward toward the water table. This will not necessarily be the case at every location or at every time. Therefore, both cases of solubility in the UZ are considered being greater and less than in the invert of the EBS.

If solubility limits are higher in the geosphere than in the emplacement drifts, then there is no effect on transport because all available radionuclides that were transported from the emplacement drift are already aqueous species.

If solubility limits are lower in the geosphere than in the emplacement drifts, then some dissolved radionuclides will precipitate there. This would reduce the amount of dissolved radionuclides available for transport in the geosphere. Subsequent cooling may increase the solubility, restoring the precipitated radionuclides to the aqueous phase; in this case precipitation would delay, but not prevent, transport of radionuclides. It is, therefore, conservative to neglect precipitation. The magnitude of this conservative approximation may be qualitatively evaluated through a comparison of the different ranges of chemical environments estimated for the engineered barrier system as compared with the UZ. The pH of waters inside the drift range from less than 5 to more than 10 (BSC 2004 [DIRS 169860], Figures 6.13-2 through 6.13-12). The evolution of water chemistry in the UZ, however, is not so broad. Near the drift the pH ranges from roughly 7 to 8.5 (BSC 2004 [DIRS 172463], Figures 6.5-12, 6.5-25, 6.5-58). Further out into the rock, the pH ranges from about 7 to 9 (BSC 2004 [DIRS 169866], Figures 6.4-11, 6.4-13, 6.4-14, 6.4-17). Given the much larger range of pH inside the drift, equilibrium solution concentrations for radionuclides inside the drift could be significantly larger than equilibrium solution concentrations in the UZ.

Solubility limits could also affect the formation of certain kinds of true colloids, such as polymeric forms of plutonium oxide (BSC 2004 [DIRS 170025], Section 6.3.1). However, these forms of colloids have not been observed to form in experiments on waste form degradation (BSC 2004 [DIRS 170025], Section 6.3.1). Furthermore, these colloids are expected to undergo formation of pseudocolloids in the near- or far-field aquifer system (BSC 2004 [DIRS 170025], Section 6.3.1) and are, therefore, excluded.

Analysis of coupled THC effects indicates that only small changes in hydrologic properties and mineralogy a result from these coupled processes (BSC 2004 [DIRS 172463], Section 6). Therefore, far-field changes are likewise expected to be small, including mineral precipitation or dissolution and alteration of minerals such as zeolites and clays. Therefore, coupled thermal-hydrologic-chemical effects on radionuclide transport properties and the effects of different solubility limits in the geosphere are excluded because they will have no adverse effects on the radiological exposures to the RMEI, or radionuclide release to the accessible environment. Section 6.1.2 explains why low consequence for specific elements of the UZ system leads to low consequence for total system performance.

Supporting Reports: Not applicable.

6.9.9 Repository-Induced Thermal Effects on Flow in the UZ (2.2.10.01.0A)

FEP Description: Thermal effects in the geosphere could affect the long-term performance of the disposal system, including effects on groundwater flow (e.g., density-driven flow), mechanical properties, and chemical effects in the UZ.

Screening Decision: Excluded–Low Consequence.

Screening Argument: Thermal-hydrologic modeling at the mountain scale has been performed using two-dimensional cross-sectional and three-dimensional dual-permeability models (BSC 2004 [DIRS 169866], Section 6.1.2). During the early part of the heating period, important TH processes occur near the emplacement drifts. The mountain-scale models are used to capture

the TH behavior at later times, when the perturbation in temperature, and fracture and matrix liquid saturation, extends over a much larger space domain compared to the drift-scale effects. These mountain-scale TH processes include repository edge effects, large-scale enhanced water and gas flow, and potential alteration of perched-water bodies. Results from the modeling indicate that the induced flow from TH processes are much smaller than changes in flow resulting from climate change at 600 and 2,000 years (BSC 2004 [DIRS 169866], Figures 6.2-10a and b, 6.3.1-18), which are included in the flow and transport models (Section 6.2.4, FEP 1.3.01.00.0A). Percolation flux maps at the top of the CHn for the ambient and thermally perturbed case (at 500 years of heating) show very similar flow patterns with the exception of reduced flow through a central portion of the waste emplacement area under the thermally perturbed case (BSC 2004 [DIRS 169866], Figures 6.3.1-16a and b). For thermal effects on chemical processes, see FEPs 2.2.08.03.0B, 2.2.10.06.0A, 2.2.10.07.0A, and 2.2.10.09.0A. For thermal effects on mechanical processes, see FEPs 2.2.10.04.0A, 2.2.10.04.0B, and 2.2.10.05.0A.

Numerical simulations of flow at 100 years and 500 years after emplacement show reduced fracture saturation and diversion of percolating water around the dryout zone (BSC 2004 [DIRS 170338], Section 6.2.2.1). Because of the flow diversion, the dryout is more extensive and longer lasting beneath the drift; this is called the “drift shadow” effect. Note that there is no water flux inside the dryout region, because fracture saturation is zero. After resaturation in 1,000 to 2,000 years, saturations below the drift remain smaller than above, because of the “shadow zone” created by the diversion of flow around the drift (BSC 2004 [DIRS 170338], Section 6.2.2.1). In general, the TH dryout and associated coupled processes will lead to an environment where radionuclide transport in the vicinity of the drift is less likely (BSC 2004 [DIRS 170338], Section 6.2.2.1.1; BSC 2004 [DIRS 172463], Section 6.5.5.3).

The effects of repository heat and the associated dryout on shallow infiltration at the surface of Yucca Mountain were investigated in CRWMS M&O (1999 [DIRS 105031]). The primary issue for thermal effects at the ground surface is the change in temperature and its associated effect on vegetation. Based on the detailed analysis of soil temperature changes documented in CRWMS M&O (1999 [DIRS 103618]), the temperature rise will have a negligible effect on vegetation, and hence on surface infiltration.

This FEP is, therefore, excluded because it will not significantly change radiological exposures to the RMEI or radiological releases to the accessible environment. Section 6.1.2 explains why low consequence for specific elements of the UZ system leads to low consequence for total system performance.

Note that the effects of thermal-hydrologic processes on drift seepage and seepage water chemistry are addressed in FEPs 2.2.07.10.0A, 2.2.07.11.0A, 2.2.08.12.0A, 2.2.10.10.0A; and 2.2.10.12.0A.

Supporting Reports: Not applicable.

Screening Argument: This FEP raises some issues already addressed in Section 6.9.7, FEP 2.2.08.03.0B and Section 6.9.8, FEP 2.2.08.07.0B. If solubility limits decrease in the geosphere so that they are lower than in the waste emplacement drifts, then some dissolved radionuclides will precipitate as water flows out of the drifts. This limits the dissolved radionuclides available for transport into the geosphere, which results in no adverse effect on performance. See also Section 6.9.6 (FEP 2.2.01.05.0A) for additional information on this subject. If solubility limits increase in the geosphere compared with the waste emplacement drift, there is no effect on transport because all available radionuclides from the source at the waste emplacement drift are already aqueous species. The effects of colloid formation are accounted for in the colloid source term (BSC 2004 [DIRS 170025], Section 6.5.2.3). Colloids are formed from the degradation of the high-level waste and spent nuclear fuel waste forms, EBS materials, and rock (BSC 2004 [DIRS 170025], Section 6.3.1). Radionuclides associated with colloids are modeled as either irreversibly or reversibly attached to colloids to encompass the broadest range of potential radionuclide-colloid interactions (BSC 2004 [DIRS 170041], Section 6.4.5). Elevated temperatures are expected to lead to fewer colloids due to the decrease in colloid stability. This is due to the greater energy of colloid motion at higher temperatures, which allows colloids to overcome the energy barrier associated with coagulation (BSC 2004 [DIRS 170025], Section 6.3.2.1). Boiling results in evaporation and this tends to increase the ionic strengths of colloid suspensions. This also leads to colloid instability due to compression of the electric double layer surrounding colloids (BSC 2004 [DIRS 170025], Section 6.3.2.1). Therefore, colloid entrainment as a result of boiling is not expected.

The effects of temperature on radionuclide sorption were evaluated in *Radionuclide Transport Models Under Ambient Conditions* (BSC 2004 [DIRS 164500], Appendix I). This evaluation focused on the radionuclides Cs, Sr, Ba (a proxy for Ra), Ce, Eu, U(VI), Np, Pu and Am (BSC 2004 [DIRS 164500], Section II.4). The effects of temperature on sorption were found to be negligible for these radionuclides, except for Sr, Np, and U(VI). For these three radionuclides the effects of increased temperature leads to increased sorption (BSC 2004 [DIRS 164500], Section I5). Therefore, the effects of temperature on radionuclide transport can be excluded on the basis of low consequence because it has no adverse effects on performance.

The thermal-chemical interactions that will occur in the repository environment have been studied with respect to effects on the seepage water entering the waste emplacement drifts (BSC 2004 [DIRS 172463]). This model explicitly captures the effects of changes in temperature, pH, Eh, ionic strength (and other compositional variables), time dependency, precipitation or dissolution effects, and effects of resaturation (BSC 2004 [DIRS 172463], Section 6.2). Changes in fracture permeabilities were found to be on the order of the natural variation in these properties (BSC 2004 [DIRS 172463], Section 6.5.5.3 and BSC 2004 [DIRS 170038], Table 6-5), with most of the substantial effects limited to regions above and to the side of the drift within about a drift diameter (BSC 2004 [DIRS 172463], Figures 6.5-39 and 6.5-40). The predicted mineral precipitation decreases permeability in the affected regions, and leads to a reduction in flow around the drift. This is conservative for both drift seepage and radionuclide transport phenomena and this FEP is, therefore, excluded because it will have no adverse effects on the radiological exposures to the RMEI, or radionuclide release to the accessible environment.

The geochemical model includes the major solid phases (minerals and glass) encountered in geological units at Yucca Mountain, together with a range of possible reaction product minerals, CO₂ gas, and the aqueous species necessary to include these solid phases and the porewater composition within the THC model (BSC 2004 [DIRS 172463], Table 6.2-2). Compositional changes were only calculated at the drift boundary for the drift-scale THC seepage model (BSC 2004 [DIRS 172463]). Results from these simulations show most compositional variations returning to unperturbed conditions in 10,000 years or less. Variations in pH (BSC 2004 [DIRS 172463], Figures 6.5-12, 6.5-25, and 6.5-58), a key compositional variable for sorption of some radionuclides (BSC 2004 [DIRS 164500], Appendix A), roughly lie within the range of variability investigated for initial porewater compositions (BSC 2004 [DIRS 172463], Table 6.2-1). Bicarbonate is found to be depressed in concentration upon water resaturation at the drift wall, as expected based on the reduced pH values at the same time period.

Results were also investigated for the Tptpl (lower lithophysal unit) model considering a range of initial porewater compositions. In this model, five different initial porewater compositions were investigated (BSC 2004 [DIRS 172463], Table 6.2-1). Peak concentrations found at the time of rewetting in both models reflect mostly the small values of the first, nonzero, liquid-saturation output. In any case, elevated concentrations are predicted only for small liquid saturations that are not subject to significant fluid movement. The improved treatment of mineral precipitation at the boiling front used in the most recent THC model for the Tptpl also results in the prediction of lower, more realistic aqueous silica concentrations than in earlier models (BSC 2004 [DIRS 172463], Figure 6.5-16). This model also predicts, upon rewetting, more rapid return to near-ambient conditions for aqueous Ca, Na, and Cl.

The findings indicate that at the drift wall, most of the significant compositional variations resulting from thermal-chemical processes are limited to low-saturation conditions over time periods that are short relative to the 10,000-year performance period. Similar magnitudes of variation in chloride and pH were found in the mountain-scale THC model results (BSC 2004 [DIRS 169866], Section 6.4.3.3.2). The magnitudes of the variations are found to be smaller at greater distances from the drift wall. As for the drift-scale study, variations in chloride are driven mainly by evaporation and are found to return to near-ambient values upon rewetting (BSC 2004 [DIRS 169866], Section 6.4.3.3.2). Variations in pH were found to lie roughly between 7 and 9, which is similar to the results for the drift-scale THC model (BSC 2004 [DIRS 172463], Figures 6.5-12, 6.5-25, 6.5-58). The most persistent change in pH is a level of about 7 in the Calico Hills (BSC 2004 [DIRS 169866], Section 6.4.3.3.2, Figure 6.4-17), but this lies within the range of pH investigated for radionuclide sorption (BSC 2004 [DIRS 164500], Appendix A). Therefore, the effects of these changes are excluded because they will not significantly change radiological exposures to the RMEI or radiological releases to the accessible environment. Section 6.1.2 explains why low consequence for specific elements of the UZ system leads to low consequence for total system performance.

Supporting Reports: Not applicable

6.9.14 Thermo-Chemical Alteration of the Calico Hills Unit (2.2.10.07.0A)

FEP Description: Fracture pathways in the Calico Hills may be altered by the thermal and chemical properties of the water flowing out of the repository.

BSC 2004. <i>D&E/PA/C IED Subsurface Facilities</i> . 800-IED-WIS0-00101-000-00A. Las Vegas, Nevada: Bechtel SAIC Company. ACC: ENG.20040309.0026.	164519
BSC 2004. <i>D&E / PA/C IED Subsurface Facilities</i> . 800-IED-WIS0-00103-000-00A. Las Vegas, Nevada: Bechtel SAIC Company. ACC: ENG.20040309.0028.	168370
BSC 2004. <i>D&E / PA/C IED Subsurface Facilities</i> . 800-IED-WIS0-00104-000-00A. Las Vegas, Nevada: Bechtel SAIC Company. ACC: ENG.20040309.0029.	168180
BSC 2004. <i>D&E/ PA/C IED Subsurface Facilities Committed Materials</i> . 800-IED-WIS0-00301-000-00B. Las Vegas, Nevada: Bechtel SAIC Company. ACC: ENG.20040318.0030.	170058
BSC 2004. <i>Development of Numerical Grids for UZ Flow and Transport Modeling</i> . ANL-NBS-HS-000015 REV 02. Las Vegas, Nevada: Bechtel SAIC Company. ACC: DOC.20040901.0001.	169855
BSC 2004. <i>Dike/Drift Interactions</i> . MDL-MGR-GS-000005, Rev. 01. Las Vegas, Nevada: Bechtel SAIC Company.	170028
BSC 2004. <i>Dissolved Concentration Limits of Radioactive Elements</i> . ANL-WIS-MD-000010, Rev. 03. Las Vegas, Nevada: Bechtel SAIC Company.	169425
BSC 2004. <i>Drift Degradation Analysis</i> . ANL-EBS-MD-000027 REV 03. Las Vegas, Nevada: Bechtel SAIC Company. ACC: DOC.20040915.0010.	166107
BSC 2004. <i>Drift Scale THM Model</i> . MDL-NBS-HS-000017 REV 01. Las Vegas, Nevada: Bechtel SAIC Company. ACC: DOC.20041012.0001.	169864
BSC 2004. <i>Drift-Scale Coupled Processes (DST and TH Seepage) Models</i> . MDL-NBS-HS-000015 REV 01. Las Vegas, Nevada: Bechtel SAIC Company. ACC: DOC.20040930.0003.	170338
BSC 2004. <i>Drift-Scale Radionuclide Transport</i> . MDL-NBS-HS-000016 REV 01. Las Vegas, Nevada: Bechtel SAIC Company. ACC: DOC.20040927.0031.	170040
BSC 2004. <i>Drift-Scale THC Seepage Model</i> . MDL-NBS-HS-000001 REV 03. Las Vegas, Nevada: Bechtel SAIC Company. ACC: DOC.20041201.0008.	172463
BSC 2004. <i>EBS Radionuclide Transport Abstraction</i> . ANL-WIS-PA-000001, Rev. 01. Las Vegas, Nevada: Bechtel SAIC Company.	169868
BSC 2004. <i>Engineered Barrier System Features, Events, and Processes</i> . ANL-WIS-PA-000002, Rev. 03. Las Vegas, Nevada: Bechtel SAIC Company.	169898
BSC 2004. <i>Engineered Barrier System: Physical and Chemical Environment Model</i> . ANL-EBS-MD-000033, Rev. 03. Las Vegas, Nevada: Bechtel SAIC Company.	169860

LB0312TSPA06FF.001. Six Flow Fields with Raised Water Tables. Submittal date: 12/23/2003.	166671
LB0406U0075FCS.002. Flow Focusing in Heterogeneous Fractured Rock: Summaries. Submittal date: 06/30/2004.	170712
LB0408CMATUZFT.002. Carbonation - Papadakis Model Calculations for Carbonation Distances. Submittal date: 08/31/2004.	172022
LB0408CMATUZFT.003. Leaching of Altered Cementitious Materials - Estimates of Molecular Diffusion/Dispersion in Cementitious Material Transport. Submittal date: 08/31/2004.	171705
LB0408CMATUZFT.004. Leaching of Altered Cementitious Materials - EQ3/6 Simulations for Cementitious Material Transport. Submittal date: 08/31/2004.	171706
LB990501233129.004. 3-D UZ Model Calibration Grids for AMR U0000, "Development of Numerical Grids of UZ Flow and Transport Modeling". Submittal date: 09/24/1999.	111475
LB990801233129.001. TSPA Grid Flow Simulations for AMR U0050, "UZ Flow Models and Submodels" (Flow Field #1). Submittal date: 11/29/1999.	122753
LB990801233129.003. TSPA Grid Flow Simulations for AMR U0050, "UZ Flow Models and Submodels" (Flow Field #3). Submittal date: 11/29/1999.	122757
LB990801233129.009. TSPA Grid Flow Simulations for AMR U0050, "UZ Flow Models and Submodels" (Flow Field #9). Submittal date: 11/29/1999.	118717
LB9908T1233129.001. Transport Simulations for the Low, Mean, and Upper Infiltration Scenarios of the Present-Day, Monsoon, and Glacial Transition Climates for AMR U0050, "UZ Flow Models and Submodels." Submittal date: 03/11/2000.	147115
LL000122051021.116. Summary of Analyses of Glass Dissolution Filtrates. Submittal date: 01/27/2000.	142973
LL020711323125.001. Pre-Test Calculations for Grout Carbonation Experiments. Submittal date: 08/13/2002.	172026
LL030211423125.005. Cementitious Grout-Seepage Water Interaction. Submittal date: 02/02/2004.	172020

gas present in the drift environment will react with any hyperalkaline plume that is generated, reducing both the solution pH and the calcium concentration to values close to ambient pore water values.

DTN: LB0408CMATUZFT.002 [DIRS 172022], which presents the results of calculations carried out with the Papadakis (2000 [DIRS 172019]) model. This model provides rates of carbonation of Portland cement as a result of the diffusion of CO₂ gas through the pores of the cement, where it reacts with the phases there to form calcite. The model assumes rates are limited by the rate of diffusion of CO₂ through the pores—no limitation based on the intrinsic rate of reaction with CO₂ is considered. In addition, the process requires that an aqueous film wetting the cementitious grain be present, since the aqueous phase is the medium in which the reaction occurs. It is possible that the Papadakis (2000 [DIRS 172019]) equation will not hold up at very low relative humidities, since in this case the aqueous film wetting the cement grains may be only partly present. Otherwise, the Papadakis (2000 [DIRS 172019]) model is a straightforward implementation of the analytical solution for gas diffusion, which then provides the rate at which the carbonation front (conversion to calcite) occurs. It is implemented here with the software Excel, which is exempt from software qualification requirements. Similar calculations were used to plan carbonation tests over a 100-day period DTN: LL020711323125.001 [DIRS 172026])—the calculations presented here use the same Papadakis model, but are extended to time scales of 50 years (Ziegler 2004 [DIRS 171694], Table D-5), with data presented in DTN: LB0408CMATUZFT.002 [DIRS 172022]). A range of input values of Portlandite cement, silica fume, and water content in the cement recipe are considered—these control the porosity of the resulting cement, which controls the rate of CO₂ gas diffusion through the pores. Also considered in Ziegler (2004 [DIRS 171694], Table D-5) are ranges in the relative humidity, which is the other control besides the porosity on the rate of CO₂ diffusion through the pores of the cement. These input parameters cover the range of likely conditions and materials to be used in the drift environment. Since the Papadakis (2000 [DIRS 172019]) model is based on a well known analytical solution to the diffusion equation and it has been calibrated independently for different cement “recipes” (the relative proportions of water, Portland cement, and silica fume), the data produced from the model can be accepted as qualified.

DTN: LB0408CMATUZFT.003 [DIRS 171705] presents calculations on the horizontal spreading of an aqueous plume as result of both hydrodynamic dispersion and molecular diffusion. The input values for these calculations are based on independently qualified data. These qualified input data are clearly identified. The calculation itself is a straightforward one based on analytical solutions to the diffusion-dispersion equation in which Fick’s Law (diffusion and dispersion is proportional to the concentration gradient) is used. The calculations were carried out with the commercial software Microsoft Excel, thus, removing the need to qualify the software.

DTN: LB0408CMATUZFT.004 [DIRS 171706] presents calculations using the qualified code EQ3/6 version 7.2b (database DATA.0) of the equilibrium phase assemblage as a function of differing calcium and silica contents of the cement. These calculations demonstrate that elevated temperatures, as are expected in the drift environment, will convert the primary assemblage of portlandite (CaOH)₂ and silica fume to other phases. These other phases, when reacted with water, will show a lower pH than would a water reacted with portlandite (Ziegler 2004 [DIRS 171694], Table D-12). This calculation assumes equilibrium conditions will prevail and

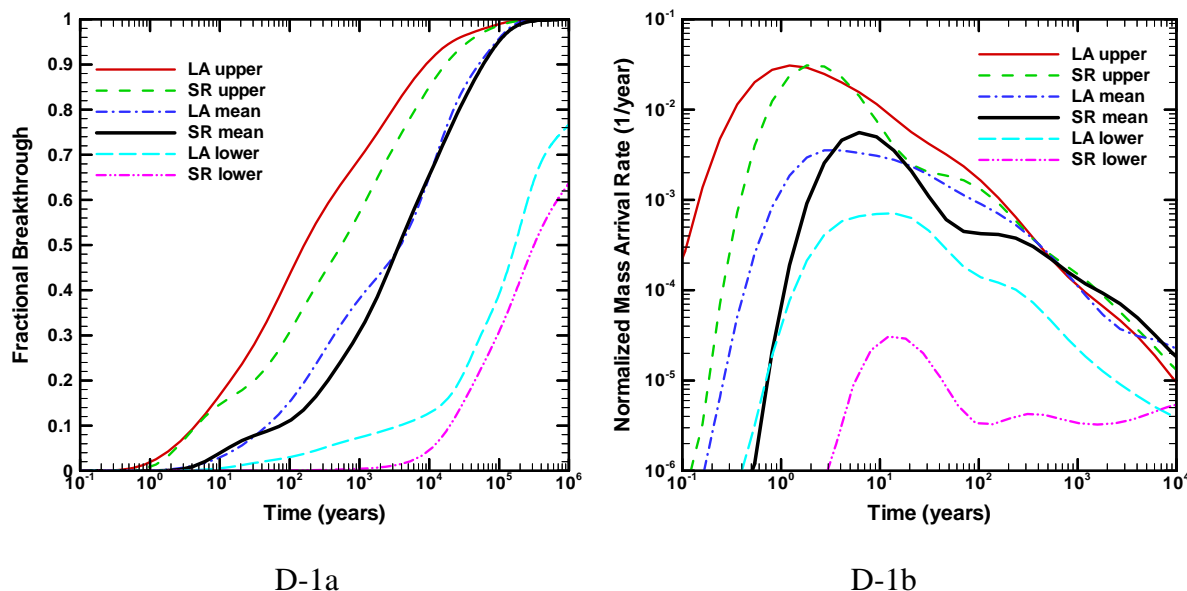
surrounding rock (Section D2.1.1). However, geologic observations are not adequate to assess the effects of some of the changes caused by fault displacements that could be important to UZ flow and transport. In particular, the effects of previous fault displacements on the present-day fracture apertures at Yucca Mountain are difficult to determine by observation. For example, it is difficult to determine by geologic observation that a given fracture with an effective hydraulic aperture of, approximately 200 μm , may have had an effective hydraulic aperture of 150 μm at some point in the past before to a fault displacement event. In fact, it is difficult to determine the effective hydraulic apertures of the present-day fractures at Yucca Mountain by direct observation (Sonnenthal et al. 1997 [DIRS 101296], Section 7.5.4). Fracture apertures at Yucca Mountain are determined through pneumatic flow tests (giving the fracture permeability) and a theoretical model relating fracture frequency (determined by observation of fractures), fracture permeability, and fracture aperture (Sonnenthal et al. 1997 [DIRS 101296], Section 7.5.4).

D3.1 USE OF SR MODEL

In this work, steady state flow fields with fracture apertures undisturbed or changed (to represent the effects of seismic activity) were first calculated, and then used to run transport simulations. A steady state flow field had previously been calculated for the SR model (CRWMS M&O 2000 [DIRS 151953], Section 6.2.1), and this result provided a flow field that could be used as an initial guess to determine the steady state flow fields for these calculations. For this reason these calculations were done using the SR model. The SR and LA models are similar enough that use of the SR model instead of the LA model is appropriate for the purpose of determining the sensitivity of transport to fracture aperture. The SR and LA flow and transport models are based on the same dual-permeability/active fracture conceptual model and numerical implementation. The main differences in the model set-up are the nonlocal connections introduced for the PTn/TSw interface between fractures and rock matrix. However, these lie above the repository and should have negligible effect on flow and transport below the repository. The most significant differences between the models is the shift in repository footprint to the north for the LA case compared with the SR design and some limited changes in parameterization based on new calibrations for the LA case.

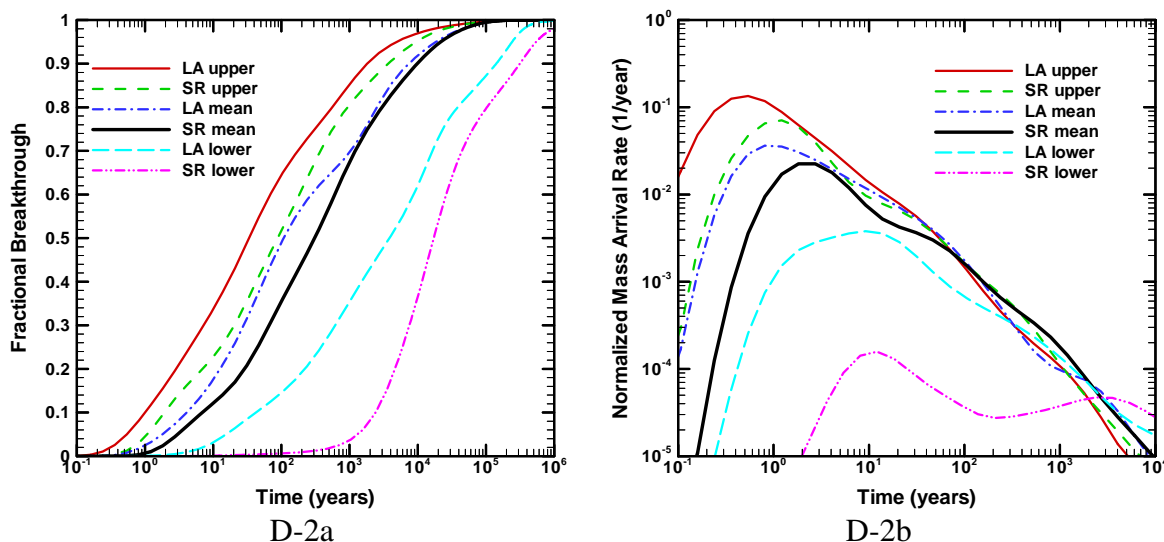
Transport results for present-day and glacial-transition climate scenarios are compared in Figures D-1 and D-2. The transport results are for a uniform, instantaneous release of tracer mass from all repository locations at time zero. The tracer is nonsorbing, but can diffuse into the matrix. The present-day scenarios are shown in Figures D-1a and D-1b, which present the fractional cumulative breakthrough curves and normalized mass arrival rate curves, respectively. (For a unit tracer released at the repository at time zero, the fractional breakthrough curve represents the tracer cumulative arrival at the water table as a function of time. The normalized mass arrival rate is the time-derivative of the breakthrough curve.) These curves show that differences between SR and LA are small in comparison with the uncertainty represented by the lower, mean, and upper infiltration scenarios for this climate. The glacial-transition scenarios are shown in Figures D-2a and D-2b, which present the fractional cumulative breakthrough curves and normalized mass arrival rate curves, respectively. Although differences between the SR and LA cases are more pronounced for the glacial-transition case, these differences are still small in comparison with the uncertainty for this climate. Furthermore, the goal of the present analysis is to compare the relative effects of changes in fracture aperture on UZ transport behavior. Given that the conceptual and numerical models for the SR and LA models are nearly the same, the

SR model should be suitable for its intended use of assessing transport sensitivity to seismic-induced changes in fracture properties.



DTNs: LB03033DUZTRAN.001 [DIRS 170372] LA transport breakthrough curves.
 LB9908T1233129.001 [DIRS 147115] SR transport breakthrough curves.

Figure D-1. Comparison of SR And LA Transport Results for an Instantaneous Release of (Nonsorbing) Tracer Mass at the Repository Horizon at Time Zero under Present-Day Climate. a) Cumulative Fractional Breakthrough, b) Normalized Mass Arrival Rate



DTNs: LB03033DUZTRAN.001 [DIRS 170372] LA transport breakthrough curves.
 LB9908T1233129.001 [DIRS 147115] SR transport breakthrough curves.

Figure D-2. Comparison of SR and LA Transport Results for an Instantaneous Release of (Nonsorbing) Tracer Mass at the Repository Horizon at Time Zero under Glacial-Transition Climate. a) Cumulative Fractional Breakthrough, b) Normalized Mass Arrival Rate